CHALMERS

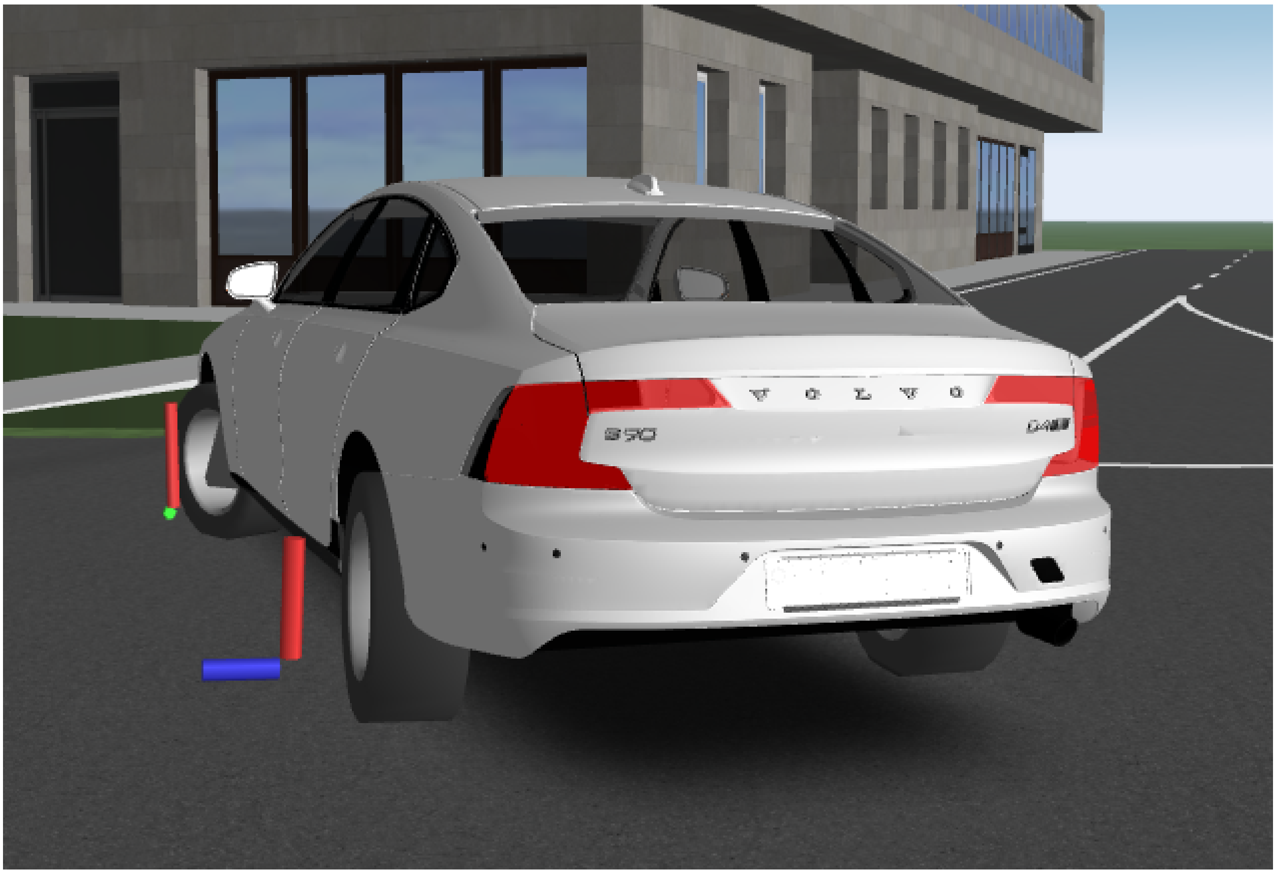

Rear Wheel Steering

A Study on Low-Speed Maneuverability and Highway Lateral Comfort

Master's thesis in Automotive Engineering

JULIETTE UTBULT

Department of Applied Mechanics
CHALMERS UNIVERSITY OF TECHNOLOGY
Göteborg, Sweden 2017

MASTER'S THESIS IN AUTOMOTIVE ENGINEERING

Rear Wheel Steering

A Study on Low-Speed Maneuverability and
Highway Lateral Comfort

JULIETTE UTBULT

Department of Applied Mechanics
Division of Vehicle Engineering and Autonomous Systems
Vehicle Dynamics Group
CHALMERS UNIVERSITY OF TECHNOLOGY

Göteborg, Sweden 2017

Rear Wheel Steering
A Study on Low-Speed Maneuverability and
Highway Lateral Comfort
JULIETTE UTBULT

Master's thesis 2017:08
Examiner: Bengt JH Jacobson
Supervisor: Matthijs Klomp
ISSN 1652-8557
Department of Applied Mechanics
Division of Vehicle Engineering and Autonomous Systems
Vehicle Dynamics Group
Chalmers University of Technology
SE-412 96 Göteborg
Sweden
Telephone: +46 (0)31-772 1000

Cover:
Volvo S90 model equipped with RWS simulated in IPG CarMaker.

Chalmers Reproservice
Göteborg, Sweden 2017

Rear Wheel Steering
A Study on Low-Speed Maneuverability and
Highway Lateral Comfort
Master's thesis in Automotive Engineering
JULIETTE UTBULT
Department of Applied Mechanics
Division of Vehicle Engineering and Autonomous Systems
Vehicle Dynamics Group
Chalmers University of Technology

Abstract

Rear wheel steering is a well-known technology that has been researched for many years but have only had limited market acceptance in niche applications. Increased urbanization and the advent of autonomous drive could change the impact of rear wheel steering in favor of greater market acceptance but in what way needs to be better understood. Low-speed maneuverability and highway lateral comfort are two attributes believed to be affected by the introduction of rear wheel steering. Lateral comfort includes comfort in the general sense with vibrations and high-frequency oscillations, but also low-frequency oscillations which may lead to motion sickness. A literature study was conducted in order to better understand the nature of motion which causes discomfort in automobiles, and means of evaluating comfort. A frequency weighting according to ISO-standard was used for comfort and a weighting found in literature was used for motion sickness in the lateral direction as this is still an unexplored area. Maneuverability was assessed using two analytical cases; curvature and swept path width, and two driving scenarios; rear-end parking and driving through a T-crossing. Two control laws were used; one feedforward and one feedback. The feedforward control law was designed to keep the body side slip angle zero at steady state cornering, and the feedback control was taken from literature with the aim of dampening yaw rate. This control law is mainly designed for stability, and was thus not used in low-speed maneuvers and only used for comparison in highway maneuvers. The angle on the rear wheels was limited to +/-5°. Rear wheel steering performed well at low speeds, improving the maneuverability by increasing the maximum curvature for a given steering wheel angle by 12% and decreasing the swept path width up to 14%. The vehicle with rear wheel steering also performed better in the driving scenarios by occupying less space during the maneuver. Overtaking and a sinus steer were the two maneuvers used to assess comfort and motion sickness. Rear wheel steering at high speeds decreased the measures of discomfort by 8.17% in the sinus steer maneuver and with 18.16% for a passenger in the rear seat, and MSDV is decreased by 7.32% in the sinus steer and by 4.04% in the overtaking maneuver for a passenger in the rear seat, implying that a vehicle equipped with rear wheel steering is more comfortable. Yaw stability was assessed as a final objective where it was shown that rear wheel steering, both the feedforward and feedback control, improved stability leading to a safer vehicle. To conclude, the results of this study implies that rear wheel steering can lead to improved maneuverability in low-speeds, improved comfort during highway driving, and improved safety in terms of stability.

Keywords: Autonomous drive, urbanization, maneuverability, lateral comfort, motion sickness.

Acknowledgements

I would like to express my greatest thanks to my supervisor Dr. Matthijs Klomp who has supported me all the way throughout this thesis through professional advice, motivational speeches and encouragement. Thank you for this golden opportunity to investigate an exciting new technology, I have learnt so much about research of automotive nature and how complex and interconnected vehicle dynamics can be.
Secondly, I would like to express my gratitude to my examiner Professor Bengt JH Jacobson at Chalmers who has given me insight and opened up my mind to adjacent technologies and new aspects.
I would also like to thank the department Vehicle Dynamics CAE at Volvo Car Group and all its members for support, companionship and insightful advice during my time there.
Finally, I would like to thank my friends and family, especially my ever-supporting, loving partner Daniel Torinsson, who has lifted me up when the project was weighing me down and celebrated my success.

Nomenclature

$\alpha_{f,r}$	Side slip angle of front or right axle [°]
β	Body side slip angle [°]
δ	Steering wheel angle [°]
δ_f	Front wheel steering angle [°]
δ_r	Rear wheel steering angle [°]
η	Understeer coefficient
μ	Friction coefficient
ω_{ref}	Yaw rate reference [$°/s$]
a_w	Frequency weighed acceleration [m/s^2]
a_y	Lateral acceleration [m/s^2]
AD	Autonomous Drive
$C_{f,r}$	Cornering stiffness at front or rear [$N/°$]
CoG	Center of gravity
d	Distance between two points [m]
$d(t)$	Disturbance
$e(t)$	Error
ESC	Electronis Stability Control
ESP	Electronic Stability Program
$F_{xf,r}$	Longitudinal force at front or rear [N]
$F_{yf,r}$	Lateral force at front or rear [N]
F_{z10}	Static vertical load front [N]
F_{z20}	Static vertical load rear [N]
FB	Feedback
FF	Feedforward
FL	Front left wheel
FR	Front right wheel
FWS	Front wheel steer
g	Gravitational acceleration [m/s^2]
$G(s)$	Process
I	Moment of inertia [kg/m^2]
k_D	Dampening coefficient
l	Length of wheelbase [m]
l_f	Distance between CoG and front axle [m]
l_r	Distance between CoG and rear axle [m]
M_z	Moment around z-axis [Nm]
$MSDV$	Motion Sickness Dose Value
$r(t)$	Desired state
r, ω_z	Yaw rate [$°/s$]

RL	Rear left wheel
RR	Rear right wheel
RWS	Rear wheel steer
SWD	Sine with dwell
T	Period time [s]
$u(t)$	Input to system
V	Velocity [m/s]
v_x	Velocity in longitudinal direction [m/s]
v_y	Velocity in lateral direction [m/s]
VCC	Volvo Cars Corporation
W_d	Frequency weighting for health and comfort in horizontal direction
W_f	Frequency weighting for motion sickness in vertical direction
W_y	Frequency weighting for motion sickness in lateral direction
$y(t)$	Output from system

Contents

Abstract i

Acknowledgements i

Nomenclature iii

Contents v

1 Introduction 1
1.1 Background . . . 1
1.2 Objective . . . 1
1.3 Limitations . . . 1

2 Theory 3
2.1 Comfort . . . 3
2.1.1 Motion Sickness . . . 3
2.1.2 Assessment of vibration . . . 5
2.2 Low Speed Maneuverability . . . 8
2.3 Control strategies . . . 10
2.4 Yaw Stability . . . 12
2.4.1 RWS vs ESC . . . 13
2.5 Autonomous drive (AD) . . . 15
2.6 Virtual Vehicle Environment . . . 16
2.6.1 CarMaker . . . 16
2.6.2 IPGDriver . . . 16
2.7 Driving simulator . . . 19

3 Methodology 20
3.1 Control strategies . . . 20
3.1.1 Vehicle model . . . 20
3.1.2 Step response . . . 22
3.1.3 RWS design: body side slip β equal to zero at steady state cornering . . . 22
3.1.4 RWS design: feedback proportional controller . . . 23
3.2 Co-simulation: CarMaker and Simulink . . . 24
3.3 Low speed maneuverability . . . 26
3.3.1 Turning geometry . . . 26
3.3.2 Driving scenarios . . . 27
3.4 Highway lateral comfort . . . 28
3.4.1 Test cases . . . 29
3.5 Yaw stability . . . 29
3.6 Driving simulator . . . 30

4 Results 31
4.1 Step response . . . 31
4.2 Low speed maneuverability . . . 33
4.3 Highway lateral comfort . . . 38
4.3.1 Frequency weighting . . . 38
4.3.2 Overtaking . . . 39
4.3.3 Sinus steer . . . 44
4.3.4 Yaw stability . . . 48
4.3.5 Driving simulator . . . 50

5 Discussion 51

6 Conclusion **55**

A Simulink: Feedforward model **59**

B Simulink: Feedback model **60**

C ISO-standard frequency weighting W_d **61**

1 Introduction

This thesis is conducted in cooperation with Volvo Cars Corporation. It aims to investigate the effect of rear wheel steering on low speed maneuverability and highway lateral comfort.

1.1 Background

Rear wheel steering, RWS, is a well-known technology that has been researched for many years but have only had limited market acceptance in niche applications. Apart from only steering the front wheels, a steering input to the rear wheels is added either through the input of the driver or through a computer for various purposes. Increased urbanization and the advent of autonomous vehicles could change the impact of rear wheel steering in favor of greater market acceptance but in what way needs to be better understood. A large part of Volvo customers live in cities, in an urban environment. Furthermore, according to the UN the world's population living in urban areas will increase from 54% in 2014 to 66% by 2050 (United Nations, 2015). With a larger urban population follows an increased pressure for space in the city. With urban streets and parking lots, follow a demand on the driver's ability to maneuver the vehicle in narrow spaces. This effort could be reduced with increased low speed maneuverability. Furthermore, McKinsey predicts that 60% of the global GDP will be generated in 600 urban centers solely by 2025 (McKinsey, 2011). Thus not only the need for this technology, but the resources required to develop and implement it, will be present in the urban areas. Additionally, with the advent of autonomous drive, AD, the driver will be relieved, to some extent, of the driving effort and the technology will be responsible for driving style and comfort. Lateral comfort is here defined as the lateral motion as perceived by the vehicle occupants as a result of path control and lateral disturbances. But as the driver is transformed into a passenger, it will become exposed to the discomforts suffered by passengers such as motion sickness. Motion sickness while performing secondary tasks is a potential challenge in the utility of autonomous drive. Lateral comfort will likely be an important factor to the success of AD. Can lateral comfort and motions behind motion sickness be improved with rear wheel steering?

1.2 Objective

The purpose of this thesis is to investigate how rear wheel steering can the improve low-speed maneuverability and highway lateral comfort using simulation and subjective investigation in an advanced driving simulator at Vehicle Dynamics CAE. Other factors that will be considered are the influence of rear wheel steering on the agility and stability of the vehicle in standard and evasive maneuvers. As a stretched target, the effects of rear-wheel steering relative to systems like torque vectoring will be considered as well. Research questions to be answered:

- How can highway lateral comfort be improved with RWS?

  What is lateral comfort?

  What motion can cause lateral discomfort?

  How can lateral comfort be modelled?

- How can low speed maneuverability be improved with RWS?

  Both in parking and driving situations.

- What is the dynamic safety benefit with RWS?

1.3 Limitations

The following limitations narrow down the scope of the thesis:

- Controller concepts that need to be implemented shall mainly be based the literature survey, as opposed to being designed within the project.

- How rear wheel steering should be mechanically and electrically integrated into VCC platforms is outside the scope of this project.
- Whether RWS is more motivated for AD or manual drive, MD, is outside the scope of this project.
- Requirements on an RWS system, such as actuators, is not to be analysed. However, actuator and angle limits on RWS should be reviewed in literature and taken into account.

2 Theory

This chapter begins with a section describing comfort that leads to a summary of different theories which causes motion sickness, both in general and in vehicles. Furthermore, the method of assessing vibration for comfort will be described and the test maneuvers used to evaluate comfort. Thereafter follows a section about maneuverability and different means of assessing it. The next section introduces some control strategies for RWS used by literature. Yaw stability is further investigated as well as RWS as a stability system compared to differential braking based yaw stability control systems such as ESP. Thereafter follows an introduction to the software used in this thesis. Finally, a short section on autonomous drive and a small introduction to driving simulators finish the chapter.

2.1 Comfort

Comfort in vehicles can be evaluated through the following main aspects: temperature, air quality, noise, vibration, light and ergonomics (da Silva, 2002). The aspect dependent on vehicle dynamics is vibration (and to some extent noise indirectly). Parsons et al performed a study on six axis vehicle vibration and its effect on comfort (Parsons et al, 1979). The results suggest that the three translational axis causes greater discomfort, and that vibrations in the vertical axis is expected to cause greatest discomfort. However, the study only includes frequencies larger than 1Hz. For occupants in a vehicle, there are two frequency ranges that should be considered; 0.5-80Hz for perception, health and comfort as well as 0.1-0.5Hz for motion sickness (da Silva, 2002). Comfort is mostly associated with acceleration and jerks. Thus by reducing these parameters, comfort is improved. Since the human body is more sensitive to vibrations at specific frequencies, frequency weightings are often used when evaluating comfort. This is further discussed in section 2.1.2.

Since comfort is dominant in the vertical direction, this is also where it is evaluated mostly. It can be improved through dampers, springs, etc. However, the lateral motion can also contribute to comfort, or rather discomfort, for passengers in the rear seat especially. Low frequency oscillations may lead to motion sickness. According to Elbanhawi et al, the root cause of motion sickness for passengers is oscillations in the lateral direction (Elbanhawi et al, 2015). The origin of this motion acting in the lateral direction is steering. Smooth control of the steering angle can reduce motion sickness and improve the overall ride quality. Steering behaviour is driver specific and hard to control. However, for autonomous cars it could be influenced. Although smooth control of the steering angle might reduce transient and high frequency oscillations in lateral acceleration, low frequency oscillations that are related to motion sickness in the vertical and lateral direction are harder to affect by present means since they depend on road grades and curvatures. In order to reduce motion sickness, the cause behind it and the motion characteristics that trigger it need to be evaluated.

2.1.1 Motion Sickness

In general

Motion sickness is a common phenomenon experienced by the majority of the population at least once in their lifetime. It involves both physical and subjective symptoms such as nausea, vomiting, drowsiness, stomach discomfort, cold sweating etc. It is called by many names based on the causation; car sickness, sea sickness and space sickness for example. In the past, the most common assumption was that motion sickness was induced by physical stimuli, but since simulators came into usage, visually induced motion sickness (VIMS) has been introduced. In this context, motion sickness is described as cyber sickness, simulator sickness and gaming sickness. It has been shown that females are more susceptible to motion sickness than males, and that the susceptibility declines with age (Paillard et. al,2013).

The reason for motion sickness is not yet fully known. According to the sensory conflict theory, which is widely accepted as the explanation for motion sickness, it will develop when the sensory information gained from the vestibular system (records spatial orientation), visual system and kinesthetic system(from muscles and joints) differ from one another (eg. sitting in a, according to the visual information, stable environment while feeling movement) or differ from the expected motion from the "internal model" built by experience (Zhang et al, 2015).

However, the traditional sensory conflict theory does not explain motion sickness produced by all conditions according to Sherman (Sherman, 2002). He states that additional sensory inputs may trigger motion sickness such as visceral gravitoceptors that may contribute to how the body determines its position. Gravitoceptors are specialized nerve endings located at various locations in the body that provide the brain with information regarding body position, gravitational forces and equilibrium (Psychology Dictionary). The postural instability theory suggests that motion sickness is caused by postural sway and the inability to actively control the body's postural motion.

A third theory is presented by Bles et al (Bles et al, 1998). The cause is defined through the subjective vertical conflict theory to the following: "All situations which provoke motion sickness are characterized by a condition in which the sensed vertical as determined on the basis of integrated information from the eyes, the vestibular system and the nonvestibular proprioceptors is at variance with the subjective vertical as expected from previous experience". This theory matches well with the findings of Förstberg where the combination of roll motion and lateral motion was found to be more nauseogenic than any of the two on its own (Förstberg, 2000). He concludes that the combination will generate a variable g-vector both in size and direction which will be in conflict with the *subjective vertical*, (SV).

The vertical is aligned with the force of gravity, as one can predict by the name. The subjective vertical is based on previous experience and expectation while the *sensed vertical* is based on the input of motion. If these two differ, according to the SV-conflict theory, motion sickness will arise. The internal model expects that the subjective vertical will be aligned with gravity always, independent of if the body is moving or stationary. Bles et al mentions the situation where a car drives a winding road at night, the rear seat passengers get motion sickness as the gravitoinertial force vector continuously changes, and the passengers do not have a clear visual of the angular motion due to the darkness and the stable visual interior of the vehicle. The SV-conflict theory explains why drivers never get motion sick as they anticipate which maneuvers come next, and why it is beneficial for passengers susceptible for motion sickness to sit in the front seat. If the subject is placed in the rotational axis, motion sickness will not arise. However, this is hardly the case for a passenger in the rear seat who experiences lateral accelerations as well as yaw and roll motion without anticipation, which can provoke motion sickness.

The different theories are intertwined and the differences are minor. Even though the mechanisms inside the body that cause motion sickness are not fully clear, the environmental excitation initiating the phenomenon in the body that is generally accepted is a sensory conflict (Golding, 2006).

In vehicles

Motion sickness is common in many different means of transportation, particularly in automobiles. With the progress of autonomous drive (AD) in passenger cars, one of the advantages is involvement in secondary tasks while riding in the vehicle. The introduction of autonomous cars would lead to the driver's loss of controllability. The driver would transform into a passenger, exposing the driver to an environment typically experienced by passengers. However, if persons particularly susceptible to motion sickness are to be able to exploit the advantages with AD, means for reducing motion sickness in vehicles need to be investigated and evaluated. In order to develop means of reduction of motion sickness, the main causation in vehicles needs to be identified.

Turner and Griffin studied the effect of driver, route and vehicle on motion sickness in public transport where the test subjects were placed in buses and coaches that were driven various routes with different drivers (Turner and Griffin, 1999). The vehicles were measured in x-, y-, and z-axis and roll, pitch and yaw. The results suggested that low-frequency lateral acceleration was primarily responsible for motion sickness. Passenger illness and nausea varied along the length of each coach providing the highest ratings at the rear of the vehicle, where the magnitudes of lateral acceleration were greatest. This increase in lateral acceleration at the rear of the coaches may be explained by centripetal effects according to Turner and Griffin. When the vehicle enters a curve, the front wheels will follow the curve path while the rear will "cut the corner", thus reducing the turning radius and increasing the lateral acceleration.

These findings correlates well with the findings of other studies. Donohew and Griffin conducted a study to evaluate the effect of frequency of lateral oscillation on motion sickness (Donohew and Griffin, 2004). In road transportation there are significant horizontal accelerations at frequencies less than 0.2 Hz. Thus, the study investigated the effect of lateral oscillation at frequencies between 0.0315 and 0.2 Hz. The test subjects were solely male that had to rate their susceptibility to motion sickness prior to the testing. The oscillation had a constant peak velocity over the frequency range and the average illness rating of the subjects increased as the frequency increased, thus with increasing acceleration magnitude. Donohew and Griffin concluded that for lateral oscillations in of the frequency range 0.0315 to 0.2 Hz, having the same peak velocity, the probability of mild nausea increases with the increase of frequency of oscillation.

Kato and Kitazaki performed a study in order to understand carsickness based on the sensory conflict theory (Kato and Kitazaki, 2006). They hypothesized that motion sickness could be mitigated by a reduction of low frequency motion. Since the vestibular and visual systems are located in the head, the magnitude of head motion seems to be related to motion sickness. Motion sickness when watching an internal screen or reading in a vehicle occurs since the signals from the otoliths (detect translational motion) and the semicircular canals (detect rotational motion) are in conflict with the visual information (eyes detect relative motion between the human body and its surroundings). Thus another hypothesis was that motion sickness due to visual motion could be mitigated by controlling the amount of stimuli to the visual organs. The results show that the motion sickness due to secondary tasks can be reduced if the relative motion between the subject and the stimuli is reduced, for example by pitch compensation of the displayed images and adjusting the image so that it is in line of sight.

2.1.2 Assessment of vibration

The effect of acceleration at different frequencies on human health, comfort and motion sickness can be evaluated through frequency weighting. To evaluate comfort and health, there are ISO-standard frequency weightings in the vertical, horizontal and rotational direction. Frequency weighting for motion sickness however can only be found in the vertical direction. The weightings for health and comfort (from now on referred to as H&C) in the horizontal and vertical direction, W_d and W_k respectively, and for motion sickness, W_f, can be seen in figure 2.1

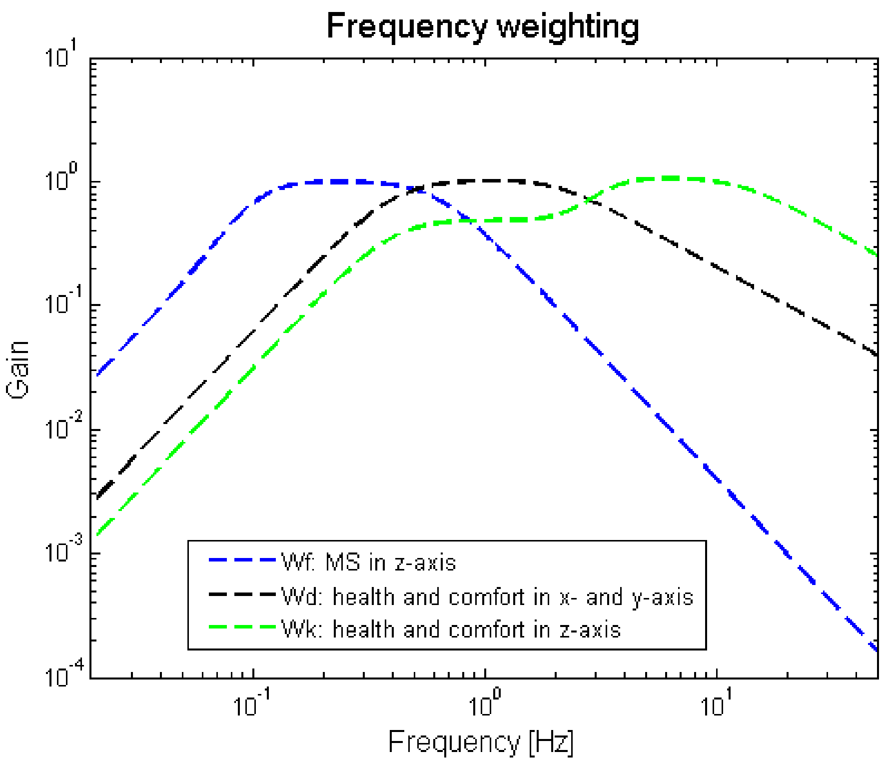

Figure 2.1: *Acceleration frequency weighting (ISO 2631-1).*

As can be depicted from figure 2.1, the weighting W_d assumes the highest sensitivity at approximately 0.5-2 Hz while the sensitivity spectrum for W_k is around 10Hz. The weighting W_f assumes highest sensitivity between 0.125-0.25 Hz, with decreasing sensitivity at lower frequencies (down to 0.1 Hz) and at higher frequencies (up to 0.5Hz) (Turner and Griffin 1999). Due to the fact that W_f is defined in the vertical direction, a Motion Sickness Dose Value, MSDV, has been used to predict motion sickness in ships where vertical oscillation is the prime causality (Donohew and Griffin, 2004). However, it has been shown that lateral oscillation has a greater effect on motion sickness than vertical oscillation in road vehicles (Turner and Griffin, 1999). Golding et al. found that horizontal motion was twice as nauseogenic as vertical motion (Golding et al., 1995). The problem is that there is no international standard that define the frequency weighting for motion sickness in the lateral acceleration. Lateral motion decreases rapidly with decreasing frequency <0.125Hz and so the standard used for vertical acceleration is less suitable for usage in the lateral direction (Turner and Griffin, 1999).

Donohew and Griffin developed a frequency weighting for lateral acceleration using the data obtained in an experiment as well as data provided by previous experiments (Donohew and Griffin, 2004). The subjects in their study were selected so as to match the motion sickness susceptibility of the subjects in an earlier study with higher frequencies. Frequency dependence of motion sickness was found by dividing the proportion of subjects reaching a given illness rating by the r.m.s. acceleration magnitude. This gives a frequency weighting and is equivalent to the 'normalized vomiting' procedure used to determine the frequency weighting of vertical acceleration. The validity of this operation is based on the assumption that the effect of acceleration magnitude on motion sickness is linear. The parameters for the developed lateral acceleration frequency weighting can be seen in table 2.1.

Table 2.1: Parameters for lateral acceleration weighting (Donohew and Griffin, 2004)

Band-limiting				a-v transition			Upward step				Gain
f1	Q1	f2	Q2	f3	f4	Q4	f5	Q5	f6	Q6	K
0.02	$1/\sqrt{2}$	0.63	$1/\sqrt{2}$	∞	0.25	0.86	∞	1	∞	1	0.55

where f_1,...,f_6 are frequencies and Q_4,...,Q_6 are resonant quality factors which belong to a transfer function that determines the overall frequency weighting using acceleration as the input parameter. The total weighting function is calculated through (ISO 2631-1):

$$H(p) = H_h(p) * H_l(p) * H_t(p) * H_S(p) \tag{2.1}$$

The transfer function is expressed as a product of several factors with different characteristics defined below.

Band-limiting (two-pole filter with Butterworth characteristic)

High pass:

$$|H_h(p)| = \left| \frac{1}{1 + \sqrt{2}\omega_1/p + (\omega_1/p)^2} \right| = \sqrt{\frac{f^4}{f^4 + f_1^4}} \tag{2.2}$$

where
$\omega_1 = 2\pi f_1$
f_1 = corner frequency, i.e. intersection of asymptotes

Low pass:

$$|H_l(p)| = \left| \frac{1}{1 + \sqrt{2}p/\omega_2 + (p/\omega_2)^2} \right| = \sqrt{\frac{f_2^4}{f^4 + f_2^4}} \tag{2.3}$$

where
$\omega_2 = 2\pi f_2$
f_2 = corner frequency

Acceleration-velocity transition (proportionality to acceleration and velocity at lower and higher frequencies respectively).

$$|H_t(p)| = \left| \frac{1 + p/\omega_3}{1 + p/(Q_4\omega_4) + (p/\omega_4)^2} \right| = \sqrt{\frac{f^2 + f_3^2}{f_3^2}} \sqrt{\frac{f_4^4 Q_4^4}{f^4 Q_4^4 + f^2 f_4^2 (1 - 2Q_4^2) + f_4^4 Q_4^2}} \tag{2.4}$$

where
$\omega_3 = 2\pi f_3$
$\omega_4 = 2\pi f_4$

Upward step (steepness approximately 6dB per octave, proportionality to jerk):

$$|H_S(p)| = \left| \frac{1 + p/(Q_5\omega_5) + (p/\omega_5)^2}{1 + p/(Q_6\omega_6) + (p/\omega_6)^2} \left(\frac{\omega_5}{\omega_6}\right)^2 \right| = \frac{Q_6}{Q_5} \sqrt{\frac{f^4 Q_5^2 + f^2 f_5^2 (1 - 2Q_5^2) + f_5^4 Q_5^2}{f^4 Q_6^2 + f^2 f_6^2 (1 - 2Q_6^2) + f_6^4 Q_6^2}} \tag{2.5}$$

where
$\omega_5 = 2\pi f_5$
$\omega_6 = 2\pi f_6$

$H_S(p) = 1$ for weighting W_d. This is determined by infinite frequencies and the abscence of some quality factors.

The frequency weighting of the acceleration is performed as follows:

$$a_w(t) = \left[\sum_i (W_i a_i)^2 \right]^{\frac{1}{2}} \tag{2.6}$$

where
a_w is the frequency-weighted acceleration, $\left[\frac{m}{s^2}\right]$.
W_i is the weighting factor for the i th one-third octave band.
a_i is the r.m.s. acceleration for the i th one-third octave band.

The vibration evaluation according to ISO 2631 should always include the weighted root-mean-square acceleration.

$$a_{w_{rms}} = \left[\frac{1}{T} \int_0^T a_w^2(t) dt \right]^{\frac{1}{2}} \tag{2.7}$$

where
$a_w(t)$ is the weighted acceleration as a function of time, $\left[\frac{m}{s^2}\right]$
T is the duration of the measurements, [s].

Furthermore, in order to assess if the evaluation method described in ISO 2631 is suitable for describing the severity of vibration in relation to its effect on human beings, the crest factor is used. The crest factor is defined as the ratio of the maximum instantaneous peak value of the frequency-weighted acceleration signal to its r.m.s. value. If it is below or equal to 9, the evaluation method is normally sufficient.

$$\text{Crest factor} = \frac{|a_{w,peak}|}{a_{w,rms}} \tag{2.8}$$

The frequency weighted accelerations are then used in different ways depending on what is being evaluated. For predicting motion sickness, the *motion sickness dose value*, MSDV, is used. It can be calculated in two ways.

1. MSDV should be determined from motion measurements throughout the full period of exposure where possible. It is then given by:

$$MSDV = \left\{ \int_0^T [a_w(t)]^2 \, \mathrm{dt} \right\}^{\frac{1}{2}} \tag{2.9}$$

where
$a_w(t)$ is the frequency-weighted acceleration, $\left[\frac{m}{s^2}\right]$

T is the total period during which motion could occur, [s].

2. The second method is used if the motion exposure is continuous and of approximately constant magnitude. Then the MSDV can be calculated from the frequency-weighted r.m.s. value determined over a short period. When using this method, an exposure duration of less than 240s should not normally be used. MSDV is calculated through:

$$MSDV = a_w T_0^{\frac{1}{2}} \tag{2.10}$$

where
a_w is the frequency-weighted r.m.s. value, $\left[\frac{m}{s^2}\right]$
T_0 is the exposure duration, [s]

For seating comfort, ISO 2631 provides values which give indications of likely reactions to various magnitudes of overall vibration total values in public transport as can be seen below. However, the reactions may differ depending on passenger expectations with regard to travel time and the type of activities passengers expect to accomplish. Furthermore, individuals perceive vibrations differently. Some are more susceptible than others, perceiving vibration magnitudes as low as $0.01 \frac{m}{s^2}$. The accelerations presented below are the W_d-weighted r.m.s. accelerations.

Less than 0,315 $\frac{m}{s^2}$:	not uncomfortable
0,315 to 0,63 $\frac{m}{s^2}$:	a little uncomfortable
0,5 to 1 $\frac{m}{s^2}$:	fairly uncomfortable
0,8 to 1,6 $\frac{m}{s^2}$:	uncomfortable
1,25 to 2,5 $\frac{m}{s^2}$:	very uncomfortable
Greater than 2 $\frac{m}{s^2}$:	extremely uncomfortable

Since the thesis aims to evaluate the difference between RWS and no RWS, absolute values are not desired, rather a comparison.

Jerk is usually also evaluated when assessing ride comfort of a vehicle. Huang and Wang evaluates two classical approaches to evaluating jerk; through its peak or r.m.s. value (Huang and Wang, 2004). They concluded that the magnitude of jerk alone could not always tell whether the ride is comfortable or not, and that one needs to consider the time exposure. The r.m.s. value correlated with the passengers comments on ride quality to 83% during durative jerk but only to 57% during transient samples. They propose a method to evaluate jerk which increases this correlation to 86% for durative samples and 77% for transient ones. The method includes a way of calculating the acceptable jerk value, AJV $[m/s^3]$, through

$$\text{AJV} = 0.004 * \text{hpj}^2 + \text{rmsj} \tag{2.11}$$

where hpj is the highest peak jerk $[m/s^3]$ and rmsj is the r.m.s. jerk $[m/s^3]$.

However, the authors stress that the method needs more validation through further experiments. Thus the r.m.s. and peak values of jerk will be evaluated and compared separately in this thesis. It is desired to keep the values low.

Literature does not provide that much information about maneuvers for assessing lateral comfort. For discomfort at lower frequencies, motion sickness, many articles use lateral oscillation of different acceleration magnitudes and frequencies and combined with roll motion. In this thesis, a overtaking maneuver and a sinus of 0.2Hz will be used as test cases for evaluating comfort.

2.2 Low Speed Maneuverability

Low speed maneuverability in vehicles is usually measured through the turning radius of the vehicle. This turning radius can be described differently. The figure below presents the most common measures.

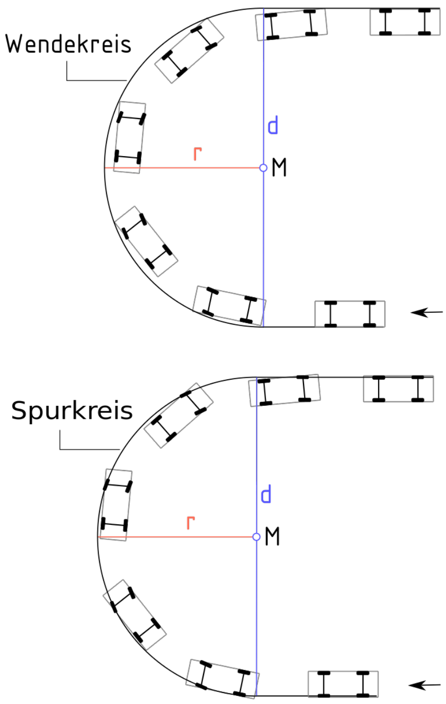

Figure 2.2: *Wall-to-wall (top) and curb-to-curb (bottom) turning radius (Wikiwand, 2016).*

The figure at the bottom represents a very common measure of turning radius; "curb-to-curb". The vehicle makes a U-turn and the turning radius is defined as the path the most outer wheel takes without hitting the curb. However, if the curb is substituted by walls this turning radius will not be enough. Thus a second measure is defined; "wall-to-wall". The vehicle once again makes a U-turn and the turning radius is defined as the path the most outer point of the vehicle takes, i.e. how far apart must the walls must be for the vehicle to complete the maneuver without making contact with them.

A third measure available is the *swept path width*, SPW, of the vehicle. It is the distance between the innermost and the outermost point on the vehicle. The swept path area, SPA, is similar but includes the area that the vehicle occupies while being maneuvered. Which measure of these two to use is less significant since the relative difference between FWS and RWS, using these two measures, will provide approximately the same information for comparison.

Marketing for low speed maneuverability usually involves parking in confined spaces. However, with the parking assistance systems available on the market this is unlikely to attract the customer's attention. Low speed maneuverability should instead be marketed through everyday driving situations in which RWS would facilitate the effort of the driver. These situations could include entering a narrow street with a lot of traffic without cutting the corner and without entering the opposite lane. An illustration of the situation can be seen in the figure below.

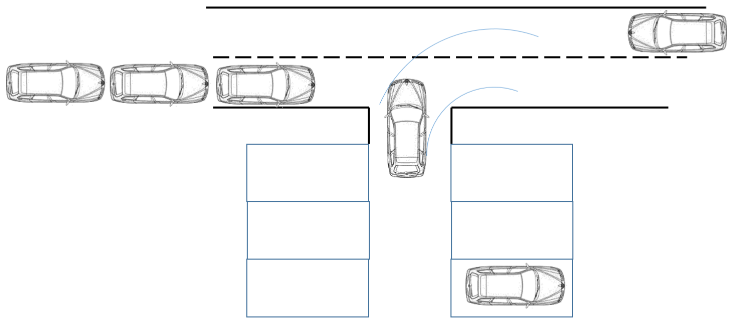

Figure 2.3: *Example of low speed manuverability; exit from a parking lot (Tobias Brandin, VCC Wheel Suspension Systems and Structures)*

2.3 Control strategies

Rear wheel steering, RWS, can be controlled either by feedforward, FF, feedback, FB (Besselink et al, 2008), (Kreutz et al, 2009), or a combination of the two (Nagai et al, 1997), (Canale and Fagiano, 2008, 2009), (Kreutz et al, 2009). The most common feedback approach uses yaw rate and/or body side slip as state variables that are compared to a reference yaw rate. Body side slip is rarely used alone since it is hard to estimate in the vehicle.

A feedback controlled system feeds back the dynamical behavior of a system for the control of a system. Usually a reference state variable is defined and the control will work to minimize the difference, the "error", between desired and actual output. A simple feedback control system can be seen in 3.4.

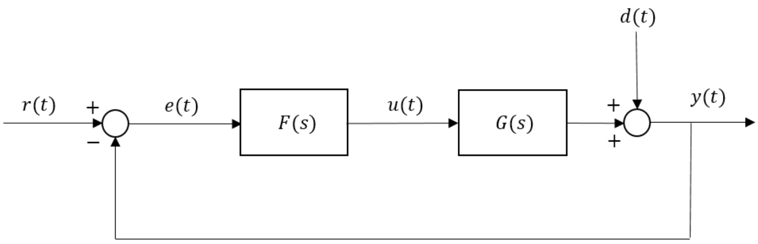

Figure 2.4: *Feedback control system*

Where r(t) is the desired state, e(t) = r(t)-y(t) is the error, u(t) is the input to the controlled system, F(s) is the regulator, G(s) is the process, d(t) is a disturbance on the sensed state and y(t) is the output. The following systems being discussed are independent, i.e. no human driver take part in the process. A feedback controlled system is stable since it will compensate for any disturbance that might occur as opposed to feedforward. However, stability of the control is a problem since it may tend to over-correct errors causing oscillations of constant or changing amplitudes if tuned poorly(Ogata, 2010).

Stability is not a problem in a feedforward controlled system. A feedforward controlled system postulates that the process being controlled is stable since the output has no effect on the control action (Lennartson, 2002) (Ogata, 2010). For each reference input there is a fixed output, therefore the accuracy of the system depends on calibration and must be re-calibrated at times. The controller is sensitive to disturbances since there are no means for compensation. Thus they can be used when the relationship between the input and output is known, and when there are no internal or external disturbances (Ogata, 2010). A feedforward control system is similar to the figure above, except that the transport of information from output to input disappears. Feedforward control has its main advantage in the fast response of output based on the input. The most desirable controller contains both systems as the combination provides both fast response, stability and insensitivity to disturbances.

Which method to use in RWS controllers depends on the function and desired outcome on the dynamics of the RWS system. If it is only desired to aid the driver in her/his maneuvers in order to improve the experience of the vehicle, then a feedforward control is enough since the driver will effectively close the loop which corrects for model errors. If the system is designed solely as an active safety system with the purpose of stabilizing the vehicle beyond the driver's control then feedback control is appropriate. However, if the RWS controller is supposed to both improve the driver's experience (which, in extreme, would be autonomous driving, AD) and function as an active safety system then the combination of feedforward and feedback is required. The following sections will provide examples for either pure feedforward or feedback, or the combination of the two in a RWS control system.

Besselink et al develops a feedback controller with the goal to minimize the yaw overshoot response to steering angle (Besselink et al, 2008). The controller looks like the following figure.

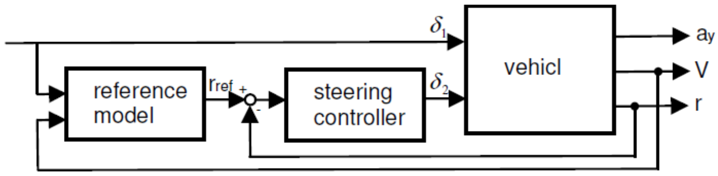

Figure 2.5: *Feedback controller (Besselink et al, 2008)*

A yaw rate reference model using front steering angle as input is compared to the actual yaw rate. The reference model has a steady state velocity gain which is dependent on the forward velocity. If the actual understeer gradient is equal to the understeer gradient of the model, no additional rear wheel steering will be required for steady state cornering. Due to this, changes in the understeer gradient due to load changes etc. will be compensated for so that the handling characteristics maintain like those of the reference model. The controller performs as expected and reduces the overshoot of the yaw rate. However, they stress that to achieve these results a very accurate signal of the yaw rate is required. The yaw rate signal used for ESP is for example too noisy and results in poor controller performance.

The second design that Besselink et al introduces is a feedforward system only. They conclude that the feedback from yaw rate is not necessary since the required rear wheel steering angle is not oscillating as the yaw rate signal is, and thus do not seem to be related. Hence, they state, it is not necessary to actively apply counter steering at the rear wheels due to yaw rate oscillation. Based on this conclusion they develop a feedforward controller presented in figure 2.6.

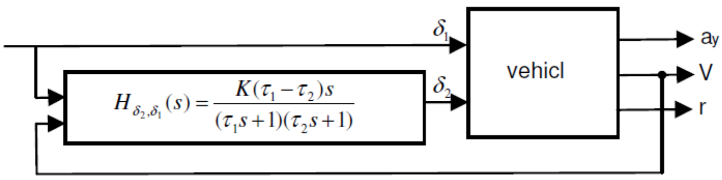

Figure 2.6: *Feedforward controller (Besselink et al, 2008)*

The controller parameters for a given velocity are determined by optimizing the yaw rate step response of the simulation model using numerical optimization techniques. As can be seen in figure 2.6 the controller is only dependent on the forward velocity. The results show that the controller is successful in reducing the overshoot of the yaw rate with an appropriate selection of parameters. Besselink et al concludes that a simple feedforward can fulfill the goal of reducing yaw rate overshoot and thus eliminated the need of an accurate yaw rate sensor. However, the article does not include the response to external disturbances such as side wind, braking on split-μ surfaces etc.

Kreutz et al presents two different control designs to a rear wheel steering system (Kreutz et al, 2009). They do not want to alter the self-steering behavior of the vehicle, thus they only want the RWS to function during transient dynamic maneuvers and not during steady state cornering. The first approach includes a classical feedback system where they wish to minimize the error between a reference yaw rate and the actual yaw rate. It is hard to find an appropriate yaw rate model that will not affect the self-steering behavior of the vehicle. The reference yaw rate can be a mathematical model of the behavior of the passive vehicle or provided by a characteristic diagram. Even though the model of the reference yaw rate is good it will never be perfect due to unknown variations in parameters in vehicle- and vehicle-road interaction they claim.

The second approach introduces feedforward control without a reference yaw rate and is not based on a mathematical model of the vehicle. It uses a mass-spring-damper system where the displacement of the mass represents the steering angle at the rear wheels. Instead of using a reference yaw rate, the yaw rate acceleration is used as an input. This is a reasonable choice since yaw rate can easily be measured in the vehicle and the yaw rate acceleration is equal to zero at steady state cornering. One advantage with this approach is that the tuning of the regulator parameters is relatively simple and universal. It does not handle split-μ situations as well as the model based controller. However, the straight line behavior is better in this controller compared to the model based, but should be further developed in order to improve comfort.

2.4 Yaw Stability

Vehicles equipped with ESC systems are required to meet performance conditions specified in the Official Journal of the EU (Official Journal of the European Union, 2015). A sine with dwell procedure produces severe oversteering which makes it suitable to be used to assess lateral stability of a vehicle equipped with the system. The test procedure can be seen in the figure below.

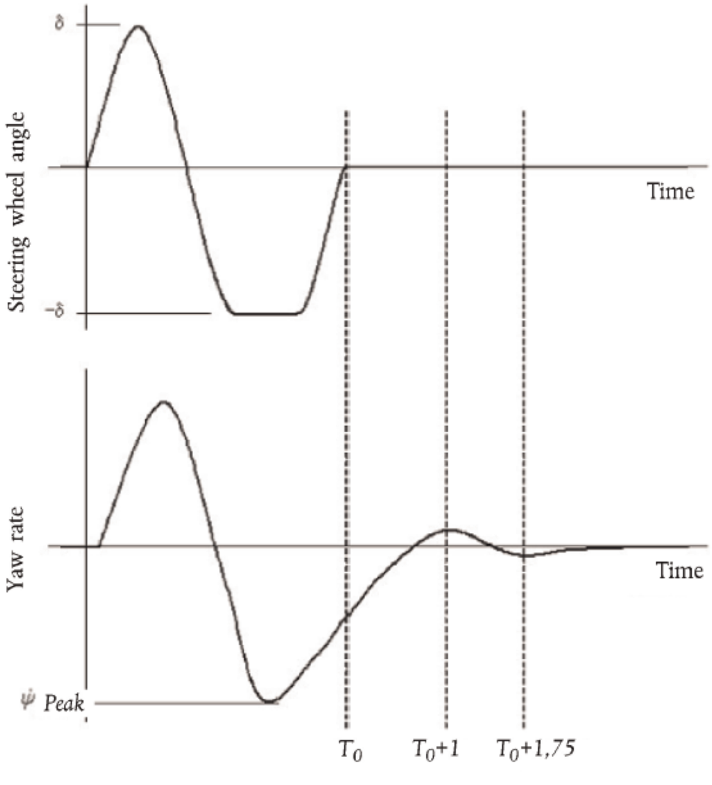

Figure 2.7: *Sine with dwell maneuver (Official Journal of the European Union, 2015).*

The requirements to be met are the following:

- The yaw rate measured one second after completion of the test shall not exceed 35% of the first peak value of yaw rate collected after the steering wheel angle changes sign.
- The yaw rate measured 1.75 seconds after completions shall not exceed 20% of the first peak value.
- The lateral displacement of the vehicle's center of gravity compared to its initial straight path shall be at least 1.83m for vehicles with gross vehicle weight less than or equal to 3500kg, and 1.52m for vehicles of greater weight when computed 1.07 seconds after the beginning of steer.

Bruzelius designed an optimal control of the steering angle of a simple vehicle dynamics model with the target to maximize yaw rate for a constant speed as this is a measure of oversteering (Bruzelius, 2015). The goal with the study was to theoretically justify the use of sine with dwell in order to assess stability. Bruzelius found that the simulated steering maneuver required to maximize the yaw rate strongly resembles the steering maneuver in a SWD. The author also evaluates the sensitivity of the maneuver, how it will change, with respect to vehicle parameters and concludes that it is very robust. It is less robust however to changes in tire and road surface properties, and thus requires skilled test drivers when performed in order to generate the desired behavior. It is also sensitive to tire stiffness, suggesting the importance of having appropriate site pressure and tire dimension. In conclusion, the SWD maneuver to assess lateral stability is theoretically well founded for a wide range of vehicles.

2.4.1 RWS vs ESC

RWS can be evaluated as a stability measure. In this thesis, the vehicle equipped with RWS is compared to a vehicle with FWS solely, no other stability systems are present. However, in 2009 it became mandatory for all new vehicles to be equipped with an ESC, electronic stability program, which stabilizes the vehicle by activating separate brakes dependent on situation (Wembley Motors, 2016). It reduces over- and understeer. Therefore a comparison between ESC and RWS is in order.

As part of an active safety system, RWS can enlarge the controllability region of the vehicle. Hoiruchi performed a study to evaluate the controllability region of chassis control systems using four wheel steering (4WS) as one of three examples (Hoiruchi, 2012).

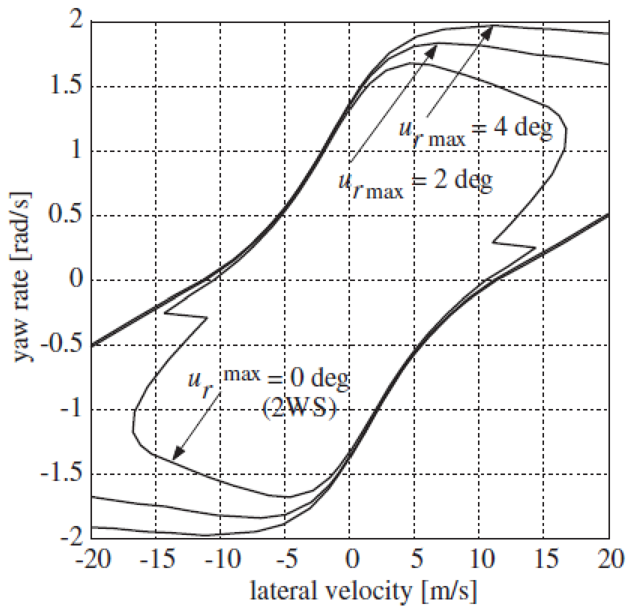

Figure 2.8: *Controllability region for 4WS (Hoiruchi, 2012)*

Figure 2.8 shows the controllability of a vehicle with additional rear wheel steering, with a maximum steering angle of 0, 2 or 4 degrees. Hoiruchi concludes that the region does not expand into the second and fourth quadrant as the lateral forces of the rear tires are saturated in these region. The enlarged controllability region will make it able for the actuators to bring the vehicle back to stability from a larger spectrum of instability as compared to only steering with the front wheels. So, active steering on the rear axle is primarily an actuator that helps reduce (transient) understeering. Hence, one could consider the mechanical design which makes the passive vehicle more oversteered. No changes to the mechanical design has been considered for the RWS vehicle in present thesis.

The controllability region of DYC, commonly known as ESC by brake, can be seen in figure 2.9 below. The region does not only expand into the second and fourth quadrant but the first and third as well. Hoiruchi then concludes that no amount of design of 4WS will enable the controller to exceed the performance of the DYC.

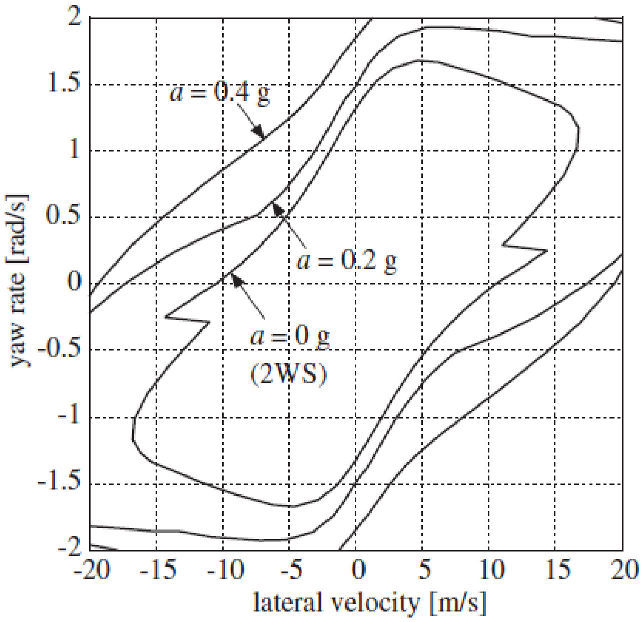

Figure 2.9: *Controllability region for DYC (Hoiruchi, 2012)*

Chatzikomis and Spentzas have concluded differently. They used four differently equipped vehicles; one with no stability systems, one with RWS, one with ESC and one with ESC and RWS combined (Chatzikomis and Spentzas, 2014). The control algorithm for RWS is a combination of feedforward and feedback. The feedforward control is based on the front wheel steering angle as well as rate of change of the same, and the feedback control tries to follow a reference body side slip angle and yaw rate. Three different tests were performed in the article; sinusoidal input where the driver was out-of-the-loop, i.e. no driver involved, an obstacle avoidance and a race track both driven by a virtual driver. The results for the sinusoidal tests show that the vehicles equipped with ESC, RWS and a combination are clear improvements compared to the vehicle without any systems. In the sinusoidal input, the equipped vehicles follow the desired trajectory almost exactly and reduce the time lags between steering wheel angle to yaw rate and lateral acceleration. This means that the vehicle will become more responsive to the driver's input.

The main objective for Chatzikomis and Spentzas of the obstacle avoidance test is to complete it with as high entrance speed as possible without knocking down any of the cones. The two secondary objectives were exit speed at the end of the maneuver and deviation from lateral acceleration and yaw rate from the desired values. The vehicles with RWS and ESC have accomplished a similar increase in initial velocity, and this is even further increased with a combination of the two systems. The vehicle with RWS has a reduced maximum side slip angle compared to ESC and a higher exit speed. This is due to the fact that ESC uses brakes as a control measure. The vehicles with the control system are returning sooner to their original lane without oscillating yaw rate compared to the unequipped vehicle. An oscillating yaw rate might lead to an uncontrollable behavior of the vehicle ultimately leading to a possible serious accident. The equipped vehicles reduce this behavior, the most successful one being the vehicle with a combination of RWS and ESC. Thus the stability of the vehicle is improved with these systems. The test track used for racing is a real-world racing track designed specifically to challenge the dynamics of a vehicle. The speed it takes to complete the track is reduced using RWS and increased using ESC given the nature of the system. The vehicle equipped with both system takes the longest time to complete the track.

Chatzikomis and Spentzas conclude that the vehicle equipped with ESC has a better capability to control stability at higher speeds by applying necessary yaw rate corrections through braking of individual wheels. The steering intervention of the rear wheels provided a smoother vehicle response by better tracking of the desired yaw rate without slowing down the vehicle, but it is limited to the amount of correction is can apply to the yaw rate. The use of a combination of RWS and ESC can reduce the amount of brake application by ESC and increase the potential of reaching the necessary corrections according to driver input.

Thus the use of RWS can augment the performance of ESC and achieve a higher level of safety for future vehicles.

Yim draws a similar conclusion from his conducted study (Yim, 2015). The study includes a performance comparison of using various combinations of AFS (active front steer), ARS (active rear steer) and when performing a DLC, double lane change. The combinations investigated are ESC, ESC+AFS, ESC+ARS, ESC+AFS+ARS and finally AFS+ARS. The criterion for passing the test is a limit in yaw rate error, the difference between a reference yaw rate and the actual yaw rate, and that the body side slip angle shouldn't be larger than 3°. The different combinations are compared to an uncontrolled vehicle apart from being compared in between. The results show that the uncontrolled vehicle doesn't pass the test while the five controlled do. All combination had similar yaw rate error during the maneuver, but other parameters differed. AFS+ARS has the lowest velocity reduction but as a side effect also the highest side slip angle due to the small error in yaw rate. This is, according to the author, a typical drawback of 4WS. The ESC equipped vehicle had the smallest side slip angle but also the greatest velocity reduction. Thus, the author concludes, ESC is necessary for a desired reduction in side slip angle to ensure stability.

2.5 Autonomous drive (AD)

Autonomous drive means that the driver is, to some extent, relieved of the driving task. There are six different levels according to SAE standards. The different autonomous levels and corresponding explanation is presented in figure 2.10.

SAE level	Name	Narrative Definition	Execution of Steering and Acceleration/ Deceleration	*Monitoring* of Driving Environment	Fallback Performance of *Dynamic Driving Task*	System Capability *(Driving Modes)*
***Human driver* monitors the driving environment**						
0	No Automation	the full-time performance by the *human driver* of all aspects of the *dynamic driving task*, even when enhanced by warning or intervention systems	Human driver	Human driver	Human driver	n/a
1	Driver Assistance	the *driving mode*-specific execution by a driver assistance system of either steering or acceleration/deceleration using information about the driving environment and with the expectation that the *human driver* perform all remaining aspects of the *dynamic driving task*	Human driver and system	Human driver	Human driver	Some driving modes
2	Partial Automation	the *driving mode*-specific execution by one or more driver assistance systems of both steering and acceleration/ deceleration using information about the driving environment and with the expectation that the *human driver* perform all remaining aspects of the *dynamic driving task*	**System**	Human driver	Human driver	Some driving modes
***Automated driving system* ("system") monitors the driving environment**						
3	Conditional Automation	the *driving mode*-specific performance by an *automated driving system* of all aspects of the dynamic driving task with the expectation that the *human driver* will respond appropriately to a *request to intervene*	System	**System**	Human driver	Some driving modes
4	High Automation	the *driving mode*-specific performance by an automated driving system of all aspects of the *dynamic driving task*, even if a *human driver* does not respond appropriately to a *request to intervene*	System	System	**System**	Some driving modes
5	Full Automation	the full-time performance by an *automated driving system* of all aspects of the *dynamic driving task* under all roadway and environmental conditions that can be managed by a *human driver*	System	System	System	**All driving modes**

Figure 2.10: *Levels of autonomous drive (SAE J3016).*

Diels and Bos mention some of the advantages with AD (Diels and Bos, 2015). A large majority of car accidents is associated with human error. By taking the driver out of the loop, the number of accidents caused by the drivers will ultimately vanish and the total number of accidents may be reduced. If AD vehicles can drive closely together, space will be freed up in the cities leading to less congestion and a more efficient traffic flow. Furthermore, the AD vehicles can be driven with high fuel efficiency leading to less pollution and better fuel economy. Apart from these environmental, economic and societal advantages, AD also makes it possible for the driver to engage in secondary tasks thus increasing the productivity of the human by utilising transport time for other value increasing activities. The higher levels of AD will transform the driver into a passenger to various degrees. However, as a passenger the driver becomes susceptible to motion sickness. Motion sickness does not only include vomiting and nausea as stated in section 2.1.1. It also includes drowsiness and many other symptoms, but most importantly as Diels and Bos mentions, it has been shown to be a risk when performing certain physical and cognitive assignments. The authors also mention that our ability to differentiate small object from one another is also affected by motion sickness. In the lower levels of *automated driving systems* the driver is still required to intervene if the vehicle can not continue for some reason. If the driver is suffering from motion sickness at the time of control transfer, a critical situation may occur. Another, great issue with autonomous drive is *trust*. Human error can be forgiven but not errors in autonomous technology. One mistake made by an AD system might bring the whole technology and its future into the shadow of mistrust. Furthermore, the driver must trust the system enough to actually engage in secondary tasks to fully enjoy what may be one major advantage with AD.

2.6 Virtual Vehicle Environment

CarMaker is a simulation software provided by IPG Automotive where a variety of automotive tests can be evaluated. The user defines a virtual vehicle environment in which a test with some objective is performed. The usage of this software is elaborated in the following sections.

2.6.1 CarMaker

A User's Guide provided by IPG describes the virtual vehicle environment which consists of the vehicle, the road and the driver (IPG User's Guide, 2016).

A *virtual vehicle* is a representative model of an actual vehicle with a behaviour to match its real counterpart. This model consists of equations of motion, kinematics, masses etc. along with other data and mathematical equations that define the multi-body system that constitutes a vehicle. The vehicle used in this thesis is a Volvo s90 which was released in mid 2016. It is a complete ADAMS/Car model which was provided by Volvo.

A *virtual road* is a modelled representation of a road, course or track which is generated for testing. The road in CarMaker can be set up using two different ways. The first way is to build the road completely from scratch through; segments, friction coefficient, width, length, slope, angle etc. Road markers and obstacles can be added as well as additional traffic and its behaviour. The second way is to use digitalized, collected data of an existing road. When the road is defined, a maneuver that the vehicle will perform need to be constructed. The maneuver is built up from different segments whose lengths are defined by time, travelled distance or an end condition. They decide the target speed, steering behaviour, gear shifting, etc. In short, the maneuver defines how the car should be driven. One can either do this by simple control, called open loop control, or let it be done by a virtual driver, called closed loop control. For example, a maneuver is to be defined where the vehicle accelerates from standstill to 100km/h. By using simple control, initially the clutch has to be released and the gas pedal pressed, then the gear change has to be defined for the appropriate speed and in combination with the clutch etc. All the gearshifts have to be defined manually. By using a virtual driver, the target speed (100km/h) solely needs to be defined and the driver will act as a real driver to a certain extent and handle the gearshifts etc. as a real driver would. There are a large variety of driver models used and more are being developed. The driver model used in this thesis is one provided by IPG Automotive and is called IPGDriver.

2.6.2 IPGDriver

The existing virtual driver in CarMaker is described in the IPG Driver User Manual 6.3, (IPG Driver, 2015). By using a driver, the vehicle model, safety system or any other objective to be investigated can be tested under more real conditions by including the reactions of a driver to the system. The module of the driver can be seen in figure 2.11.

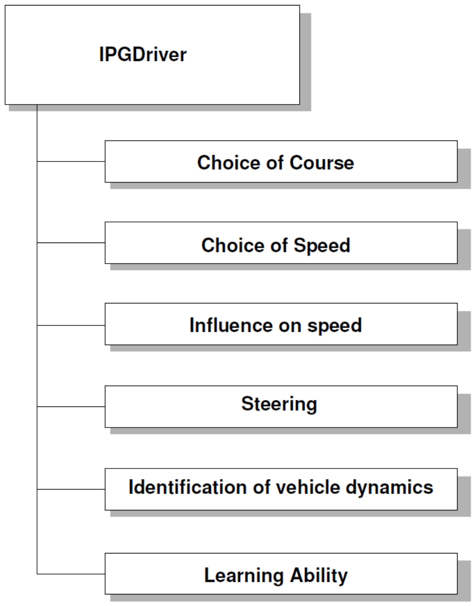

Figure 2.11: *IPGDriver Module (IPG Driver, 2015).*

- Choice of course: the driver is free to choose course within the lane boundaries. A cornering cutting coefficient can be defined in order to constrain the lane boundaries. This means that the driver must drive within the lane to different degrees depending on the cornering cutting coefficient. It can have a value between 0 and 1. If it is set to 1, the driver is completely free to cut the lanes, if it is set to 0 the driver must remain within the lane.
- Choice of speed: the driver is free to choose driving speed according to course and vehicle behaviour.
- Influence on speed: the driver can influence the selected input speed by use of gas, brake and clutch pedal as well as gear selection.
- Steering: the driver is to freely use the steering wheel.
- Identification of vehicle dynamics: in order for the driver to be able to handle the vehicle, it has automatic adaption by identifying the vehicle's behaviour.
- Learning ability: the driver is able to learn which provides the possibility to use gained knowledge from the present simulation in future simulations. This part of the driver can be activated or deactivated, and it is not used in this thesis.

The input and output parameters for the IPGDriver can be seen in figure 2.12.

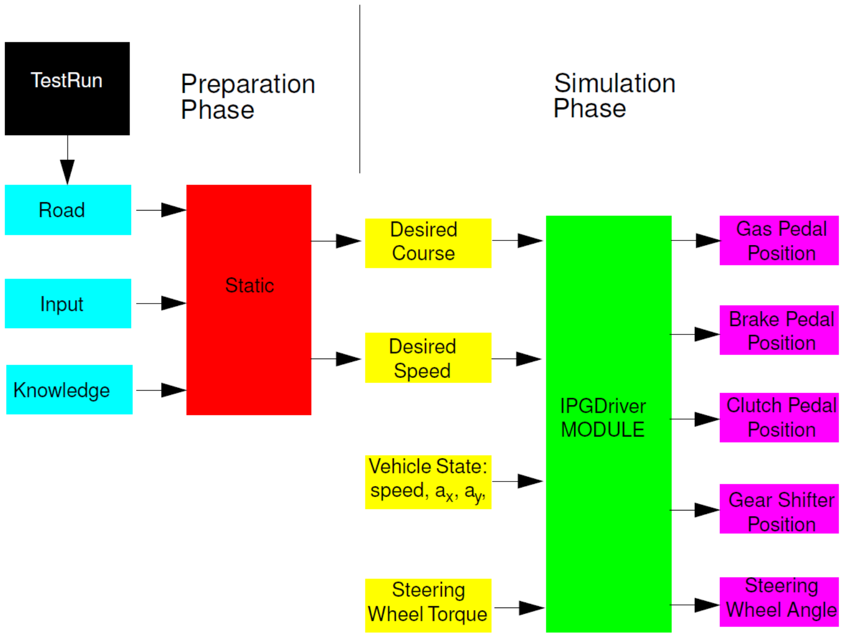

Figure 2.12: *Input parameters and state variables for IPGDriver, (IPG Driver, 2015).*

In the preparation phase, the test run is defined through definition of road, maneuver and vehicle model. Knowledge can be used if the learning ability is activated. The input parameters to the driver are listed and explained below.

- Desired course: the data that defines the road (x-,y-coordinates, width, etc.) is modified to fit the profile of the driver. For example, if the driver is to use the whole surface of the road instead of strictly following the centerline, the course would be changed accordingly (i.e. if cornering cutting coefficient is set to 1).
- Desired speed: the speed profile is determined for the course, including decelerations before cornering, accelerating after cornering, desired cruising speed etc. The driver will try to maintain the pre-defined target speed (or if no target speed is defined, it will choose the pre-determined cruising speed of the driver) but it will correct it if events occur that require it.
- Vehicle state: includes all information about current motion of the vehicle (eg. accelerations, velocity, slip angles, yaw rate etc.)
- Steering wheel torque: information provided by the vehicle model. If the torque exceeds a certain minimum value it would indicate a low of vehicle control.

The output parameters can be seen in figure 2.12. The IPGDriver module performs calculations in two steps. The first step is initialization which include desired course and desired speed. This step occurs pre-simulation. The second step is continuous during simulation and includes correction in speed, steering wheel angle and other measures that are required for the driver to follow the desired course and reach the desired speed.

There are some parameters that can be changed in order to change the driver model. These parameters include cornering cutting coefficient as mentioned earlier, cruising speed, rate of change for pedals, max longitudinal and lateral acceleration and longitudinal deceleration... In this thesis, the parameters are kept as they were assigned by default except for the cornering cutting coefficient. This was changed to 0 in order to limit the driver as much a possible by narrowing the boundaries of the lane. The difference in driving between FWS and RWS should be minimized and limiting the driver is one measure of trying to accomplish this.

2.7 Driving simulator

The definition of a simulator is *“a device that enables the operator to reproduce or represent under test conditions phenomena likely to occur in actual performance”* (Merriam-Webster, 2017). A driving simulator will try to reproduce driving characteristics and physical phenomena likely to occur during the same maneuver in real life. It can be used either for entertainment or professional purposes. The latter is usually more complex than the first. They are highly useful in research as advanced driver assistance systems, ADAS, under development can be tried, tweaked and further developed before implementing them in a physical test vehicle. Thus, the usage of a driving simulator will save both time and money during the development process.

The driving simulator at VCC can be seen in figure 2.13.

Figure 2.13: *Driving simulator at VCC.*

Driving simulators are also used in research to model driver behaviour and responses for development of active safety systems. Ordinary and critical situations can be tried in a safe environment.

3 Methodology

In this chapter, the method used for evaluating low speed maneuverability and highway lateral comfort will be described. Initially, the vehicle model used for this thesis will be presented along with its equations of motion. Thereafter follows a step response and the derivation of the control strategies. The control laws are implemented into Simulink to be used in a simulation software called CarMaker. The parameters required to perform the simulation will be presented, and then follows the methodology for low-speed maneuverability, highway lateral comfort and yaw stability. Finally, the use of the driving simulator at Vehicle Dynamics CAE will be described.

3.1 Control strategies

3.1.1 Vehicle model

The first thing to to is to decide on a vehicle model and derive the equations of motion that will lay the foundation for the control laws. The chosen model is a one-track model with the following assumptions:

- Constant velocity. Longitudinal forces can then be neglected.
- Small angles.
- Linear region of the tyres.
- Neither longitudinal nor lateral vertical load transfer is considered.

The one-track model can be seen in figure 3.1.

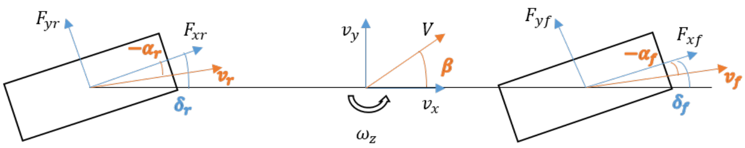

Figure 3.1: *One-track model.*

The equations of motion are derived below.

$$\sum F_y : m(\dot{v}_y + v_x\omega_z) = F_{yf} + F_{yr} \tag{3.1}$$

$$\sum M_z : I\dot{\omega}_z = F_{yf}l_f - F_{yr}l_r \tag{3.2}$$

As mentioned above, constant velocity is assumed so longitudinal forces can be neglected. Assuming small angles and that the tyres are the in linear region, the lateral force can be expressed as below.

$$F_y = C_i \arctan \alpha_i \tag{3.3}$$

Where C_i is the cornering stiffness which is constant and α_i is the slip angle at axle i. The equations for finding the slip angles are defined as follows

$$\tan(\delta_f - (-\alpha_f)) = \frac{v_y + l_f\omega_z}{v_x} \tag{3.4}$$

$$\tan(\delta_r - (-\alpha_r)) = \frac{v_y - l_r\omega_z}{v_x} \tag{3.5}$$

Using the above standing equations for 3.4 and 3.5 and small angle approximation will provide the following simplified equations for slip angle.

$$\alpha_f = -\delta_f + \beta + \frac{l_f\omega_z}{V} \tag{3.6}$$

$$\alpha_r = -\delta_r + \beta - \frac{l_r \omega_z}{V} \tag{3.7}$$

By putting equations 3.6 and 3.7 into 3.1 and 3.2, the equations of motion will become 3.1.3.

$$\dot{\beta} = -\left(\frac{C_f + C_r}{mV}\right)\beta + \left(\frac{C_r l_r - C_f l_f}{mV^2} - 1\right)\omega_z + \frac{C_f}{mV}\delta_f + \frac{C_r}{mV}\delta_r \tag{3.8}$$

$$\dot{\omega}_z = \left(\frac{C_r l_r - C_f l_f}{I}\right)\beta - \left(\frac{C_f l_f^2 + C_r l_r^2}{IV}\right)\omega_z + \frac{C_f l_f}{I}\delta_f - \frac{C_r l_r}{I}\delta_r \tag{3.9}$$

The above standing equations 3.8 and 3.12 can be rearranged using a state space model which is defined through the following two equations.

$$\dot{x}(t) = Ax(t) + Bu(t)$$

$$y(t) = Cx(t) + Du(t) \tag{3.10}$$

The states $x(t)$, the inputs $u(t)$ and the outputs $y(t)$ are

$$x(t) = \begin{bmatrix} \beta \\ \omega_z \end{bmatrix} \qquad u(t) = \begin{bmatrix} \delta_f \\ \delta_r \end{bmatrix} \qquad y(t) = \begin{bmatrix} a_y \\ \beta \\ \omega_z \end{bmatrix}$$

The outputs can be expressed in terms of the states through

$$a_y = \dot{v}_y + V\omega_z$$

$$\beta = \frac{v_y}{V}$$

The matrices for the state space model then become

$$A = \begin{bmatrix} -\left(\frac{C_f + C_r}{mV}\right) & \frac{C_r l_r - C_f l_f}{mV^2} - 1 \\ \frac{C_r l_r - C_f l_f}{I} & -\left(\frac{C_f l_f^2 + C_r l_r^2}{IV}\right) \end{bmatrix} \qquad B = \begin{bmatrix} \frac{C_f}{mV} & \frac{C_r}{mV} \\ \frac{C_f l_f}{I} & -\frac{C_r l_r}{I} \end{bmatrix}$$

$$C = \begin{bmatrix} -\frac{C_f + C_r}{m} & \frac{C_r l_r - C_f l_f}{mV} \\ 1 & 0 \\ 0 & 1 \end{bmatrix} \qquad D = \begin{bmatrix} \frac{C_f}{m} & \frac{C_r}{m} \\ 0 & 0 \\ 0 & 0 \end{bmatrix}$$

Matlab provides a function, *ss(A,B,C,D)*, which creates a state space model from above standing matrices. When the model is set up, one can derive the transfer functions using *tf* whose input is the previously acquired state space model. The result is a matrix with the transfer functions from each input to each output. In this case, it contains six transfer functions as there are two inputs and three outputs.

The block diagram of a system with both FWS and RWS can be seen in figure 3.2.

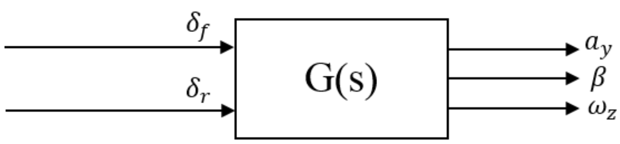

Figure 3.2: *Block diagram of FWS and RWS system without controller on RWS.*

3.1.2 Step response

A step response is a measure of seeing how the output behaves when the input is a step function. From the step response, one can extract the rise time, settling time and peak amplitude, thus providing the responsiveness and oscillatory behaviour of the system. A step response of the system with FWS only, additional FF RWS and FB RWS is performed. It was desired to have a clean system, and not a transfer function with controller included. The state space model without any controller on RWS, defining the rear wheel angle simply as an input, was derived. This approach makes it easier to change the controller without having to derive the state space model multiple times.

A common step response of a vehicle contains front wheel angle as input and yaw rate as output. It will also be used in this case. The transfer functions from front and rear wheel angle to yaw rate is taken from the matrix containing all transfer functions. The system then become a MISO system; multiple-input-single-output. To find the combined effect of the two inputs on the output, the following formula can be used.

$$Y(s) = \begin{bmatrix} G_1(s) & G_2(s) \end{bmatrix} \begin{bmatrix} U_1(s) \\ U_2(s) \end{bmatrix} = G_1(s)U_1(s) + G_2(s)U_2(s) \tag{3.11}$$

where $U_1(s)$ and $U_2(s)$ is $\mathcal{L}(\delta_f)$ and $\mathcal{L}(\delta_r)$ respectively, and $G_1(s)$ and $G_2(s)$ are the transfer functions from respective input to the output $Y(s)$ which is $\mathcal{L}(\omega_z)$ in this case. The transfer functions are put into a *transfer function* blocks, and the above standing relation is created. A step function is added as input in order to create a step response.

There is an ISO-standard for a step steer input for passenger vehicle which will be used alongside the ideal step input where the step is instantaneous. The ISO-standard states that the time for the increase from 10 to 90% of the final value should not exceed 0.15s and that the lateral acceleration should be either 2,4 or 6 m/s^2 (ISO-7401). The ideal step response is realixed using a step-function in Simulink.

3.1.3 RWS design: body side slip β equal to zero at steady state cornering

A common and basic control system for RWS is designed so as to keep the body side slip angle zero at steady state cornering. This results in a feedforward controller. Initially a one-track model is used in order to derive the equations of motion which will further be needed when deriving the control laws.

$$\dot{\beta} = a\beta + b\omega_z + c\delta_f + d\delta_r \tag{3.12}$$

$$\dot{\omega}_z = e\beta + f\omega_z + g\delta_f + h\delta_r \tag{3.13}$$

Where

$$a = -\left(\frac{C_f + C_r}{mV}\right) \qquad e = \frac{C_r l_r - C_f l_f}{IV}\Big)$$

$$b = \left(\frac{C_r l_r - C_f l_f}{mV^2} - 1\right) \qquad f = -\left(\frac{C_f l_f^2 + C_r l_r^2}{IV}\right)$$

$$c = \frac{C_f}{mV} \qquad g = \frac{C_f l_f}{I}$$

$$d = \frac{C_r}{mV} \qquad h = -\frac{C_r l_r}{I}$$

The RWS control will be designed to provide zero body side slip at steady state cornering, which means that β, $\dot{\beta}$ and $\dot{\omega}_z$ are equal to zero. Equations 3.12 and 3.13 will then become

$$0 = b\omega_z + c\delta_f + d\delta_r \tag{3.16}$$

$$0 = f\omega_z + g\delta_f + h\delta_r \tag{3.17}$$

Rearranging 3.16 and 3.17

$$\delta_r = K_{SS}\delta_f \tag{3.18}$$

Where K_{SS} is the proportional coefficient for the RWS angle and is defined as

$$K_{SS} = \frac{(bg - fc)}{(fd - bh)}$$

Since the controller does not include any feedback component, it is a feedforward controller and can be seen in figure 3.3.

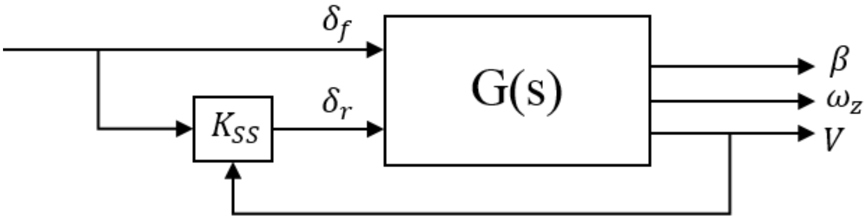

Figure 3.3: *Block diagram of feedforward K_{SS} and controlled system.*

The feedforward control law is implemented by building the coefficient K_{SS} through Simulink blocks. The velocity is read through Read CM Dict and put into the equation. Additional constants needed are defined in a Matlab-script that is run prior to the simulation. The resulting coefficient is then multiplied by the front left and right wheel to produce the rear left and right wheel angle respectively, thus to some extent preserving the relative steering ratio between the left and right wheels. The resulting angles are then defined as external rotations to the rear wheels. K_{SS} varies with velocity as is shown in figure 4.4 in the Results chapter.

3.1.4 RWS design: feedback proportional controller

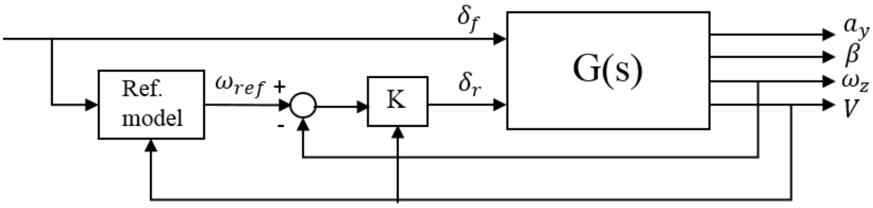

Figure 3.4: *Block diagram of feedback controller and controlled system G(s).*

The feedback control is realized by a P-regulator that regulates the error between the actual yaw rate and a yaw reference. It can be seen in 3.4 The input to the system is the driver's steering wheel angle input. This input will produce a yaw rate reference that the actual yaw rate will be compared with. The yaw rate reference is defined by

$$\omega_z = \left(\frac{1}{\frac{l}{V} + \eta \frac{V}{g}} \right) \delta_f \tag{3.19}$$

where l is length of the wheelbase, g is gravity ($9.81\left[\frac{m}{s^2}\right]$), V is velocity in $\left[\frac{m}{s}\right]$, δ is the steering wheel angle [rad] and η is the understeer gradient. The reference yaw rate needs to be limited so that the controller does not try to correct the vehicle to do something that is not possible. It is limited through

$$\omega_{lim} = \left| \frac{g\mu}{V} \right| \tag{3.20}$$

where g is gravity, V is velocity and μ is the friction coefficient. This is model based, using the model assumption that front and rear axle reaches friction limit at the same ω_z.

Thus, the yaw rate reference is defined as

$$\omega_{ref} = \begin{cases} \left(\frac{1}{\frac{l}{V}+\eta\frac{V}{g}}\right)\delta & \text{if } \omega_{ref} \leq \omega_{lim} \\ \omega_{lim} & \text{if } \omega_{ref} > \omega_{lim} \end{cases} \tag{3.21}$$

The understeer gradient is defined as

$$\eta = \frac{C_f}{F_{z10}} - \frac{C_r}{F_{z20}}$$

where C_f and C_r are the cornering stiffness at the front and rear respectively, and F_{z10} and F_{z20} are static vertical load at the front and rear respectively.

The understeer gradient η can be tuned for different purposes. It can be tuned to preserve the self-steering behaviour of the vehicle, i.e. the rear wheels will only be active in transient conditions and not in eg. steady state cornering. Another way is to tune it so that the vehicle behaves in a certain way at all times, i.e. if the vehicle is to oversteered it can be tuned to be more understeered. However, then the rear wheels will be active in most situations and will alter the self-steering behaviour of the vehicle. The understeer coefficient is set to 0 in order to strive for a neutral steered vehicle.

The gain of the regulator is defined by

$$K = \frac{l}{V} - k_D \tag{3.22}$$

where l is the length of the wheelbase, V is the velocity and k_D is a damping coefficient. Different values for k_D is investigated to find the most optimal one in combination with the chosen yaw rate reference. This gain was taken from Ackermann and Sienel (Ackermann and Sienel, 1993).

3.2 Co-simulation: CarMaker and Simulink

The simulation software CarMaker produced by IPG as described in section 2.6 and Matlab Simulink will be used for simulation. The two programs will work simultaneously in a so called co-simulation. Co-simulation is used since Simulink has a good and clear overview of all the different parameters used in the control laws which is deemed highly useful. It also provides a good way of monitoring the signals sent into CarMaker which makes it easy to detect errors in the simulink block model of the control laws as opposed to using RT Expressions in CarMaker directly. CarMaker provides a generic Simulink model as can be seen in figure 3.5.

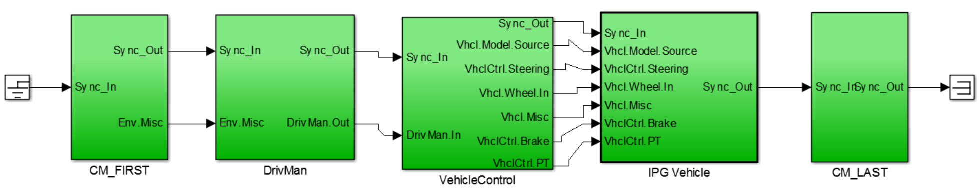

Figure 3.5: *Generic Simulink model.*

The control laws are implemented in the VehicleControl block and can be seen in appendix A and B. This is where the parameters such as driver steering wheel angle which is used in the feedback control law can be found. In-simulation parameters such as vehicle speed and yaw rate can be read through Read CM Dict block which is found in the CarMaker library for Simulink. To further overwrite an existing variable, Write CM Dict is used. If a new variable is defined, the block Define CM Dict must be used in combination with Write CM Dict.

CarMaker only allows a limited number of variables to be overwritten by the user. In this case, the steering angle on the rear wheels cannot be altered directly. Instead, an external rotation is applied to the rear wheels which will serve the same purpose as altering the steering.

Initially, a vehicle model needs to be chosen for simulation. Parameters and measures of the chosen model then need to be identified for the two control laws. The model used in this project is Volvo s90 which was released mid 2016. The model was provided by Volvo and simply needed to be added in the simulation software. The vehicle data can be seen in table 3.1.

Table 3.1: Vehicle data

Parameter	**Value**
Vehicle mass, m	1914kg
Wheelbase length, l	2.941m
Front axle distance to CoG, l_f	1.2780m
Rear axle distance to CoG, l_r	1.6630
Radius of gyration, k	1.5
Moment of inertia, I (=mk^2)	$4306.5\frac{kg}{m^2}$

Measures such as wheelbase, position of centre of gravity and mass are predefined. Additional parameters such as cornering stiffness and static, vertical load however needs to be found through simulation and calculation presented in the following paragraphs.

In order to find C_f and C_r, a test is performed where the vehicle is driven in a curve with constant radius while increasing velocity and steering wheel angle until the vehicle is no longer able to hold the curve. The side forces and slip angles are recorded. For simplification, each axle is treated as one tire, meaning that the side force and slip angle are calculated through:

$$F_{y,i} = \frac{F_{yl,i} + F_{yr,i}}{2}$$

$$\alpha_i = \frac{\alpha_{l,i} + \alpha_{r,i}}{2}$$

where i is the number of the axle, 1 or 2 for front or rear respectively.
Side force F_y is plotted as a function of slip angle α and the cornering stiffness can be found through

$$C_i = \frac{dF_{y,i}}{d\alpha_i}|_{\alpha=0}$$

Since the simulation data is not perfect, some adjustments need to be made to find the slope at $\alpha = 0$. It is done by trial and error until the lines representing the slope is deemed to fit well enough with the simulation data.

Static, vertical load is calculated through

$$F_{zi0} = \frac{mg(l - l_i)}{l}$$

The angle range of the rear wheels should be bounded as there is a limited amount of space at the rear in a passenger vehicle. A maximum 5 degrees is to be used as this was also used by some vehicle manufacturers. The rear wheel angles are bounded through a *saturation* block in Simulink. Since the steering of the rear wheels is modeled by prescribing the angle, as opposed to a more realistic model with a force or torque actuator, there is no limit to how fast the wheels can rotate. This must be constrained in the simulink model through a *rate limiter* block. Håbring tries three different types of actuators with varying performance; 10, 25 and 40°/s and concludes that a rate of 25°/s on the rear wheels will suffice in order for them to work desirably (Håbring, 2006). Thus the rate on the rear wheels is limited to 25°/s.

3.3 Low speed maneuverability

Low speed maneuverability was tested in two different kinds of test cases; turning geometry and driving scenarios. The analytical test cases are defined to assess the curvature and swept path width of the vehicle. The driving scenarios are used in order to assess the usability of RWS in everyday driving situations, i.e. putting the analytical results into a context. Only the FF controller will be used since the FB controller is designed to follow a reference yaw rate, much like an ESP system, and is more suited for stability tests.

3.3.1 Turning geometry

Curvature

The turning radius is required to find the curvature of the vehicle. In this test, the turning radius of the vehicle is defined at CoG. The purpose is to compare the difference between FWS and additional RWS for the same vehicle and thus it matters less if it is curb-to-curb, wall-to-wall etc. as long as the same measure is used for all cases. The centre of gravity was used instead. There is an existing parameter in CarMaker that records the turning radius at CoG and this measure was therefore chosen.

The turning radius for every SWA and the minimum turning radius achievable is found by slowly increasing the SWA at a small velocity so that side slip can be neglected. This maneuver is performed for FWS and RWS with 3, 5 and 7° maximum rear steer angle. The spectrum of maximum rear steer angle will provide an idea how much effect the limit of the RWS has on maneuverability. The maximum SWA achievable by the virtual driver is 630°. The target SWA (800°) exceeds this limit in order to ensure obtaining the maximum turning angle (hence minimum turning radius) for the investigated vehicle.

The curvature of the vehicle is then found through

$$\kappa = \frac{1}{R} \tag{3.23}$$

where R is the turning radius at CoG which exists as a parameter in CarMaker.

Swept path width

The most outer wheel will trace out the largest radius that the vehicle follows and the most inner wheel will trace out the smallest radius. The difference in radii, i.e. the space in between, is called the swept path width, or path width for short. The trajectory of the wheels are derived from the positions in the x- and y-direction which are provided by CarMaker through existing parameters. The parameters are defined in the global frame, i.e. with respect to where the vehicle starts in the simulation.

The wheels which will trace out the largest and smallest curve radii will be the outer front wheel and inner rear wheel respectively. The wheels will thus have different y-, and x-positions in the global frame, meaning that they will not be perpendicular to each other in any direction. Figure 3.6 presents an illustration of the path width.

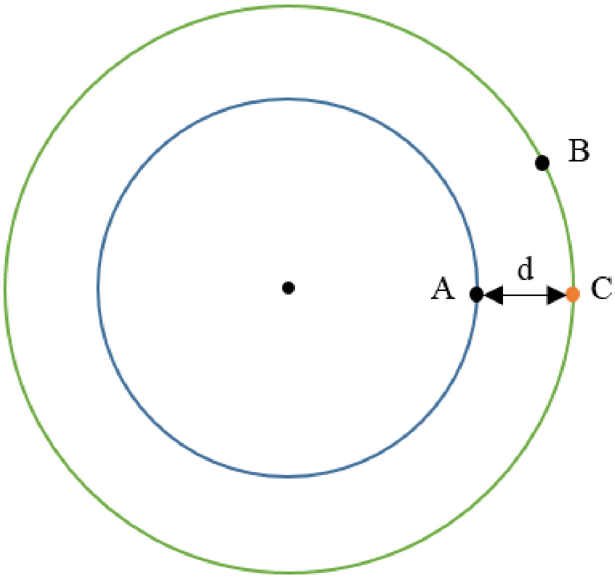

Figure 3.6: *Swept path width.*

The vehicle in the figure drives counter-clockwise around the center. Point A represents the inner rear wheel, point B represents the outer front wheel, and point C represents the desired position of the outer front wheel that will provide the distance, i.e. the swept path, of the vehicle. The swept path can be calculated through the distance formula

$$d = \sqrt{(x_1 - x_2)^2 + (y_1 - y_2)^2} \tag{3.24}$$

In order to find the smallest distance between the two, a distance vector is created which includes the distances between all the values of the inner radius and a fixed value of the outer radius. The swept path will then be the minimum value of this vector.

3.3.2 Driving scenarios

Rear end parking

There was a predefined test case in CarMaker for rear end parking where the vehicle enters a parking lot from a road, and reverses into a parking space. The only modifications made to the existing test case were to increase the width of the entrance to the parking lot and reduce the widths of the parking spaces. The parking spaces were initially 3m wide which is above the minimum of 2,5m according to Trafikverket (Trafikverket, 2004). Thus the width was reduced to 2,5m. A visualization of the rear end parking can be seen in figure 3.7.

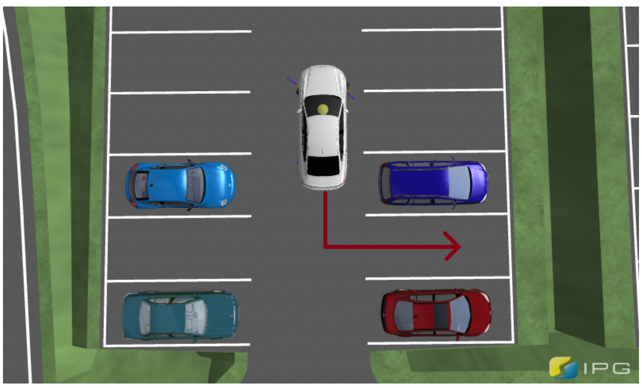

Figure 3.7: *Rear end parking maneuver.*

This test case was designed around the vehicle equipped with RWS. The maneuver was altered through trial and error in order to reach the desired one. The vehicle will park between two other vehicles by reversing into the parking space. The vehicle equipped with FWS will start reversing at the same spot using the same steering wheel angle as the one equipped with RWS. Thus the two vehicles will be provided the same initial conditions. The analysis of this test will be done visually. The maneuver can be seen in figure 3.8.

Figure 3.8: *T-crossing maneuver.*

T-crossing

Driving through a T-crossing was chosen as a dynamic maneuver to further explore the usability of RWS apart from parking. This maneuver was chosen after discussion with Tobias Brandin at VCC Wheel Suspension Systems and Structures, who identified it as a problematic situation. The test case is defined so that the vehicle will drive up to a T-crossing, stop, and then perform the turn. The width of the driving lane is 3m, which is the lowest limit recommended by Trafikverket (Trafikverket, 2002). The choice of the narrowest lane width is motivated through the desire to use the most critical situation as this is where a dangerous situation is most likely to occur and where RWS would have the largest impact. The analysis of this test will also be done visually.

3.4 Highway lateral comfort

Comfort is evaluated using both the frequency weighting W_d for health and comfort as well as the derived frequency weighting W_y for motion sickness in the horizontal direction. Lateral acceleration will vary depending on measurement position due to rotation around the vertical axis. This means that yaw motion will contribute to lateral acceleration in places separated from the vertical axis of rotation. Body sensors able to detect position, velocity and acceleration in x,y, and z-direction are placed in the rear and front seat in order to capture the environment for both driver and passenger. For comfort analysis the acceleration signal is used.

The frequency weightings are derived using the transfer functions 2.1 to 2.5 in section 2.1.2. A frequency spectrum is defined and used as input to the transfer functions among other parameters. The input to the transfer functions for W_d can be found in appendix C. The input to the transfer functions for W_y are found in 2.1 in section 2.1.2. However, since f3, f5 and f6 are equal to ∞, H_t and H_S are set to 1 according to ISO 2631.

The lateral acceleration signal is divided into its frequency components using Fast Fourier Transform (fft(*signal*) in MATLAB). The components are then multiplied with belonging frequency weighting at each specific frequency. The resulting frequency distribution is transformed back into an acceleration signal using inverse fast fourier transform (ifft(*signal*) in MATLAB). The r.m.s. value is taken from the signal through the following equation first introduced in 2.1.2.

$$a_{w_{rms}} = \left[\frac{1}{T} \int_0^T a_{W_d}^2(t)dt \right]^{\frac{1}{2}}$$

where
$a_{W_d}(t)$ is the W_d-weighted acceleration as a function of time, $\left[\frac{m}{s^2}\right]$
T is the duration of the measurements, [s].

The MSDV is then calculated through the following equations as presented in section 2.1.2

$$MSDV = \left[\int_0^T a_{W_y}^2(t)dt \right]^{\frac{1}{2}}$$

where a_w is the frequency weighted acceleration signal according to W_y.

Comparability between the two vehicle configurations can be complicated. In order to be able to compare, without error, the results from the vehicle with FWS only and from the vehicle with additional RWS, the vehicle must follow the **exact** same path at the **exact** same speed. This is hard to control as the virtual driver is free, to some extent, to choose path and speed. It is even hard to achieve when using a steering robot. Therefore, it was decided to use a ratio, a discomfort ratio, between the lateral acceleration at CoG and lateral acceleration at the driver's and passenger's seat respectively, thus normalizing the data. This way, the two vehicle configurations can be compared without necessarily having to take the exact same path at the exact same speed.

The discomfort ratio is calculated through

$$\text{Discomfort ratio} = \frac{a_{W_{d,CoG}}}{a_{W_{d,pass/driver}}} \tag{3.25}$$

where $a_{W_{d,CoG}}$ is the weighed r.m.s. lateral acceleration at CoG, passenger's or driver's seat.
The ratio for MSDV is calculated in the same manner.

$$\text{MSDV ratio} = \frac{MSDV_{CoG}}{MSDV_{pass/driver}} \tag{3.26}$$

The greater the ratio, the greater the discomfort. Furthermore, the jerk at the passenger's and driver's seat will be investigated and compared using peak and r.m.s. values and evaluated through the discomfort ratio in the same manner as the weighed r.m.s. lateral acceleration and MSDV.

3.4.1 Test cases

Two test cases were defined to assess comfort. The first one simulates an overtaking on a highway and was chosen as it is a common driving maneuver. The test case was already defined by IPG and was only slightly altered in terms of speed. The second test case is a sinus steer at 0.2Hz where MS is said to be most prominent. In order for the results to be comparable, the same lateral acceleration was to be used for FWS and RWS. This acceleration was set to 0.3g. The corresponding SWA is found through a simulation where the driver slowly increases the SWA. This simulation needs to be run for each separate controller and FWS. The data is post-processed in MATLAB and the angle is found.

3.5 Yaw stability

Stability is tested through a SWD maneuver. There is a preparatory test prior to the maneuver which is made in order to decide the steering wheel angle associated with a lateral acceleration of 0.3g at 80km/h with an increasing rate of steering wheel angle of 13.5deg/s. Steering wheel angle data and lateral acceleration is collected and imported to MATLAB where the analysis takes place. The angle, A, associated with 0.3g is taken out and used for further simulation.

Two series of sine with dwell tests are performed; one with initial clockwise steering, and one with initial counter clockwise steering. The tests will start with a steering wheel angle amplitude of 1.5A and will increase 0.5A for every test in the series until a termination criterion is reached. The termination criterion is defined when the steering wheel amplitude reaches 6.5A or 300°. If it reaches 6.5A and the amplitude is less than 270°, the final test is performed using an angle of 270°.

A test is passed if the three criteria presented in section 2.4 are met.

3.6 Driving simulator

Objective measures of comfort and maneuverability will be assessed in CarMaker, but a subjective assessment is done in the driving simulator at VCC. The FF control law is implemented into the driving simulator in order to experience the dynamics of an all wheel steered vehicle. The derived FF control law is transferred to the software Car RealTime, which is used by the simulator. Some minor alterations are needed in order for it to work properly with the platform.

The aspect investigated in the simulator is highway lateral comfort as low speeds are problematic in the simulator for the time being. Experienced test drivers will drive the simulator and assess the experience. The drivers will be allowed to drive as they wish on a three-lane highway. The cabin used in the simulator is a half-vehicle without a co-driver seat.

4 Results

The results will be presented in the following chapter. Firstly, the step response of the FF and FB control laws and the FWS system will be presented. Thereafter follows the results for low-speed maneuverability including both turning geometry and driving scenarios. Then the comfort and MSDV results will be presented for both the overtaking and the sinus steer. Finally, the yaw stability results can be found as well as the subjective experience gained from the simulator.

4.1 Step response

The two developed control laws was evaluated in a step response where the step takes place at t = 1s and the following yaw rate and lateral acceleration response can be seen in figures 4.2 and 4.1. The two figures for each metric represent an ideal step response and an ISO step response.

The response in lateral acceleration can be seen in figure 4.1.

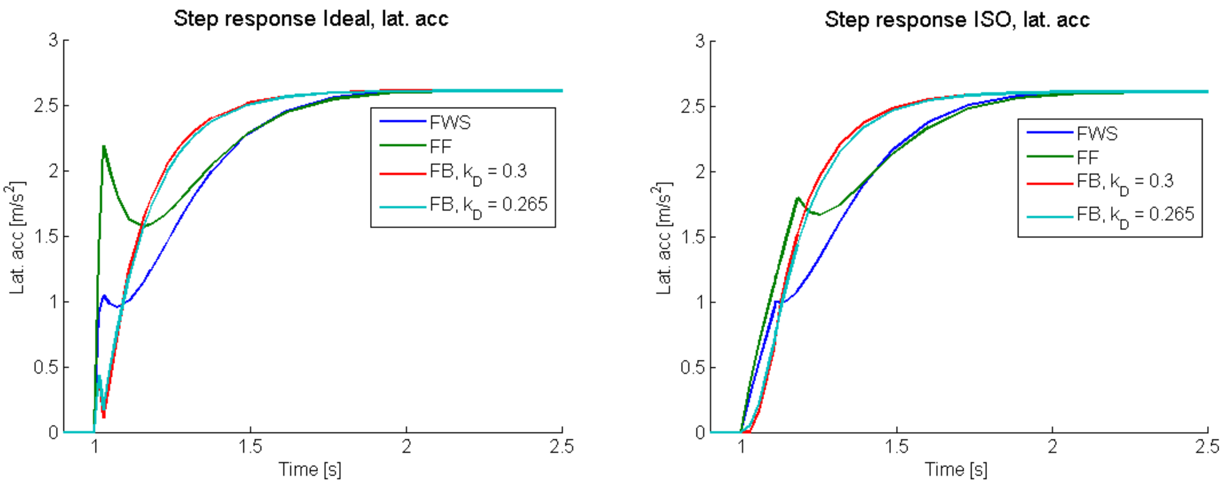

(a) *Ideal step input.* (b)

Figure 4.1: *Lateral acceleration response of a one track model for FWS and RWS, both FF and FB control laws.*

In the left figure, the response to an ideal step input is presented and in the right figure the response to an ISO step input. The lateral acceleration for FWS and RWS FF builds up fast only to decrease after approximately 0.1s and then build up more slowly. RWS FF will reach a higher acceleration peak than FWS before dropping. The RWS FB controller does not create as large initial peak but reaches its steady state value faster than the other two configurations. The ISO response is calmer as the step is ramped up. The initial peak for FWS and RWS FF is smaller and the lateral acceleration builds up in what seems to be a more controlled manner. The same applies to the RWS FB configuration.

The response in yaw rate can be seen in figure 4.2.

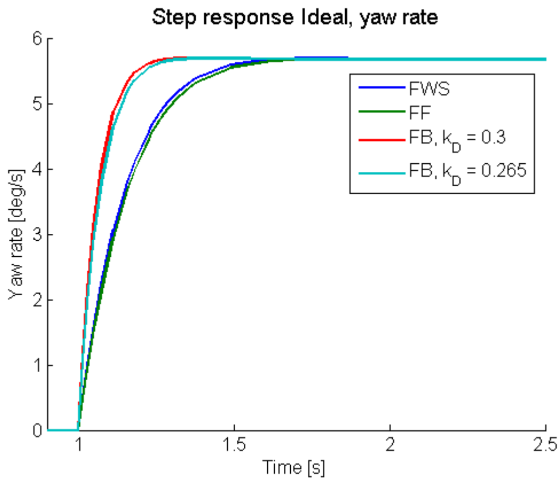

(a) *Ideal step input*

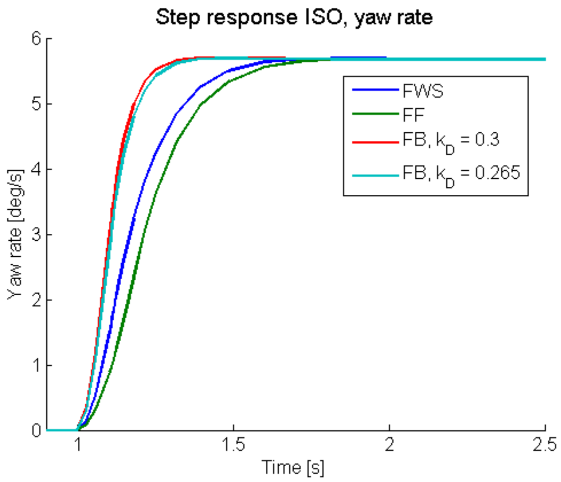

(b) *ISO step input*

Figure 4.2: *Yaw rate response of a one track model for FWS and RWS, both FF and FB control laws.*

The ideal step is presented in the left figure and the ISO step is presented in the right. Studying the figure, one can see that the FF controller increases phase lag slightly and dampens the peak amplitude. The FB controller increases the responsiveness of the model but the peak of the response is higher. The larger the dampening coefficient k_D, the faster the response. One can see that the response to the ISO step is slightly slower and enhances the above mentioned characteristics for the different configurations.

The frequency response can be seen in figure 4.3 below. The RWS FB controller has a higher gain than the other two controllers, and remains its gain over higher frequencies before it decreases. The phase follows the same trend. The difference between the RWS FF and FWS vehicle configurations is larger, RWS FF having lower gain but the phase is approximately the same.

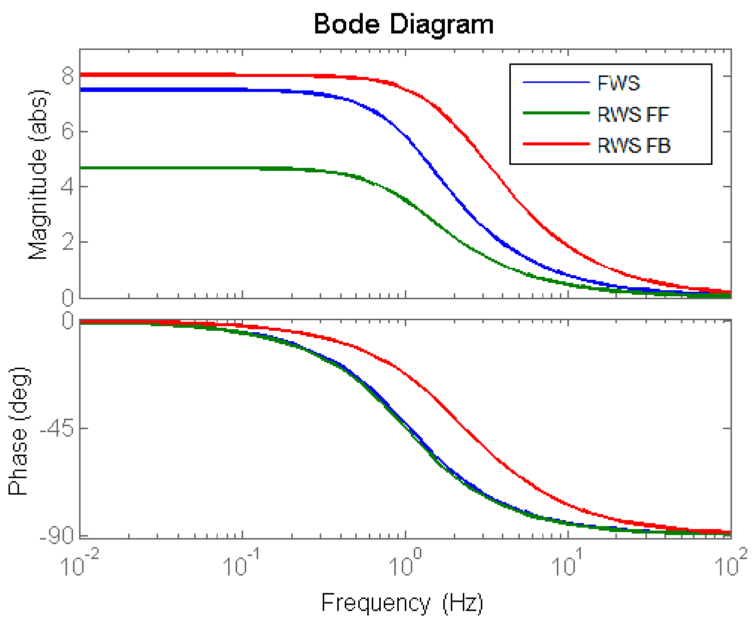

Figure 4.3: *Yaw rate frequency response to FWS, RWS FF and RWS FB with* $k_D = 0.265$.

The coefficient in the FF controller that is multiplied with the front wheel angle and ultimately produces the rear wheel angle, the FF coefficient, is dependent on velocity as can be seen in figure 4.4. At speeds below approximately 12m/s, the coefficient is negative resulting in the rear wheels being steered in the opposite direction of the front wheels. As the velocity passes 40km/h the coefficient becomes positive and the rear wheels will be steered in the same direction as the front wheels.

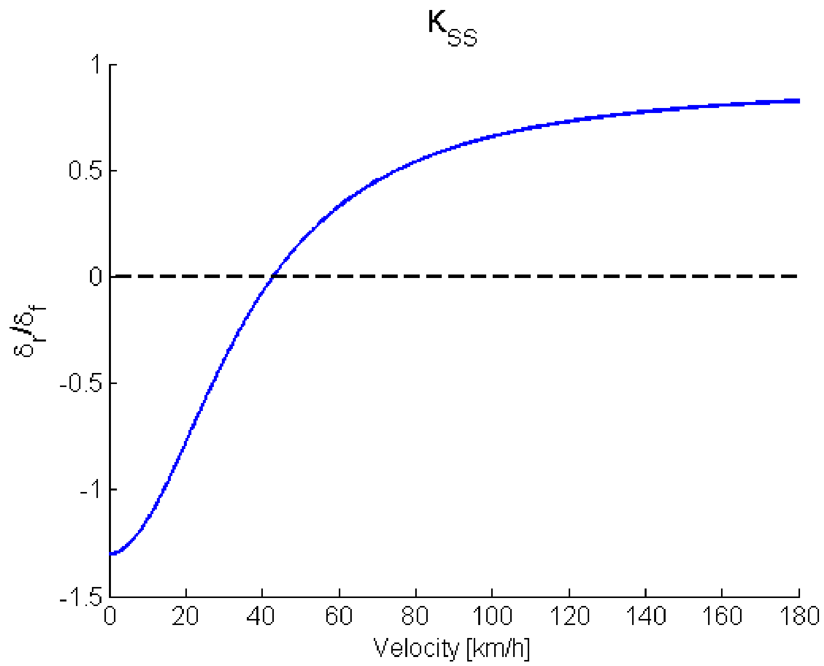

Figure 4.4: *FF coefficient as a function of speed.*

In the FB controller, the dampening coefficient was found by trial and error in the yaw stability testing according to how well the controller performed. Two values were used depending on actuator; for $10^{\circ}/s$ and 25 $^{\circ}/s$, k_D was set to 0.265 and for $40^{\circ}/s$, k_D was set to 0.3.

4.2 Low speed maneuverability

The curvature of a vehicle with FWS and RWS is presented in figure 4.5 by defining the curvature as a function of SWA.

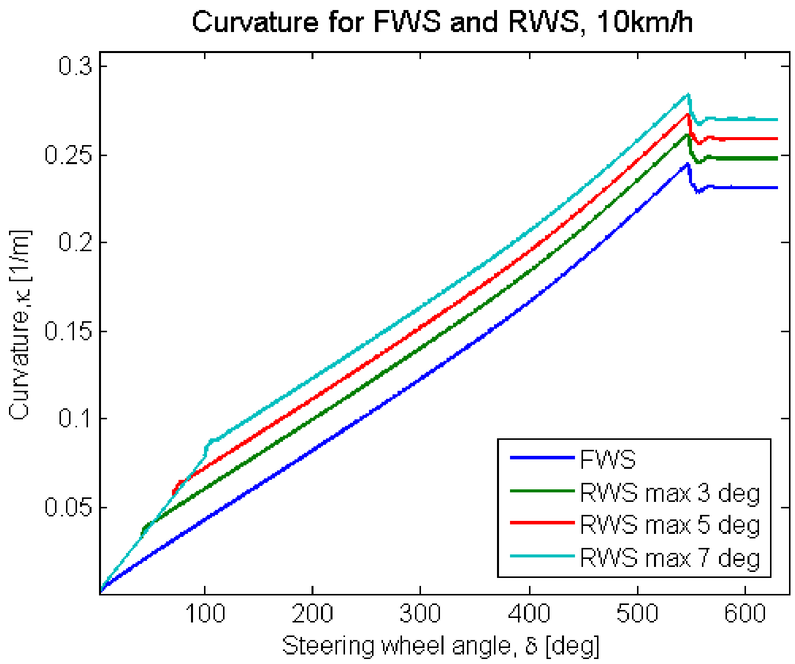

Figure 4.5: *Curvature as a function of steering wheel angle.*

As can bee seen in figure 4.5, a larger curvature can be reached with the same steering wheel angle for RWS compared to FWS. Furthermore, a vehicle equipped with RWS can reach a greater maximum curvature, thus a smaller turning radius, for maximum steering wheel angle compared to FWS. The increase in curvature for the maximum steering wheel angle and a maximum rear wheel angle of 5° is 12%. The maximum curvature of RWS increases as the maximum angle on the rear wheels increases.

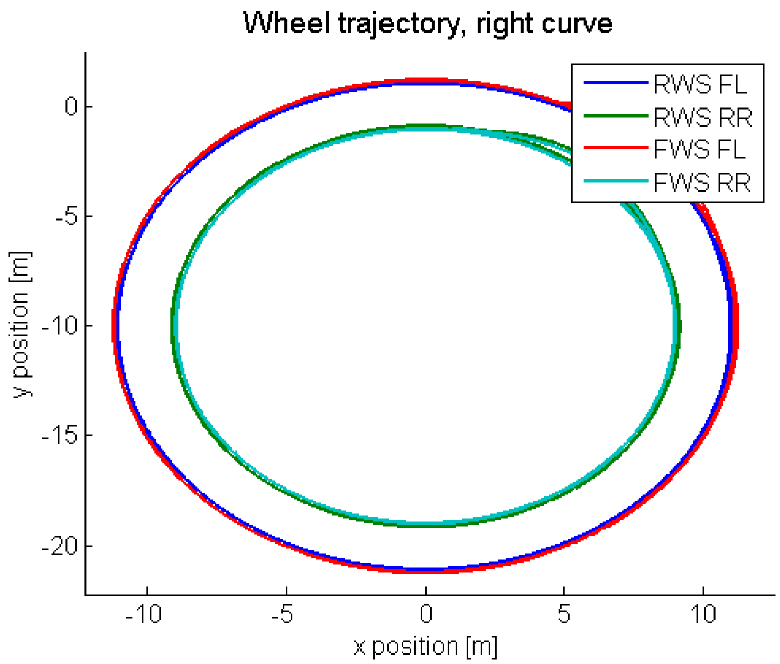

Figure 4.6: *Trajectory of most inner and most outer wheel for FWS and RWS, 10km/h, 10m curve radius.*

Figure 4.6 shows the trajectory of the most inner and most outer wheel while following a 10m radius right at 10km/h for a vehicle equipped with RWS and with FWS only. In both cases, the most inner wheel tracing out the smallest radius is the rear right wheel and the most outer wheel tracing out the largest radius is the front left wheel.

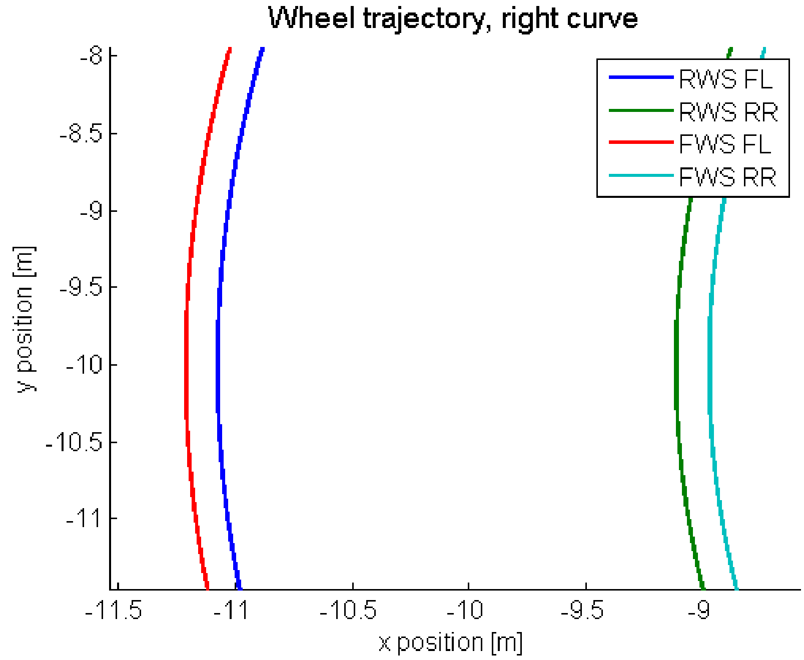

Figure 4.7: *Zoom of trajectory of most inner and most outer wheel for FWS and RWS.*

Figure 4.7 presents a magnification of figure 4.6. In this figure, the swept path width can be extracted. The swept path width is defined as the difference between the most inner and most outer point on the vehicle. The dark blue and the green curves represent the front left and rear right wheel for RWS, and the red and light blue curves for FWS respectively. As can be seen, the track width is smaller for RWS than for FWS, thus occupying less space while turning.

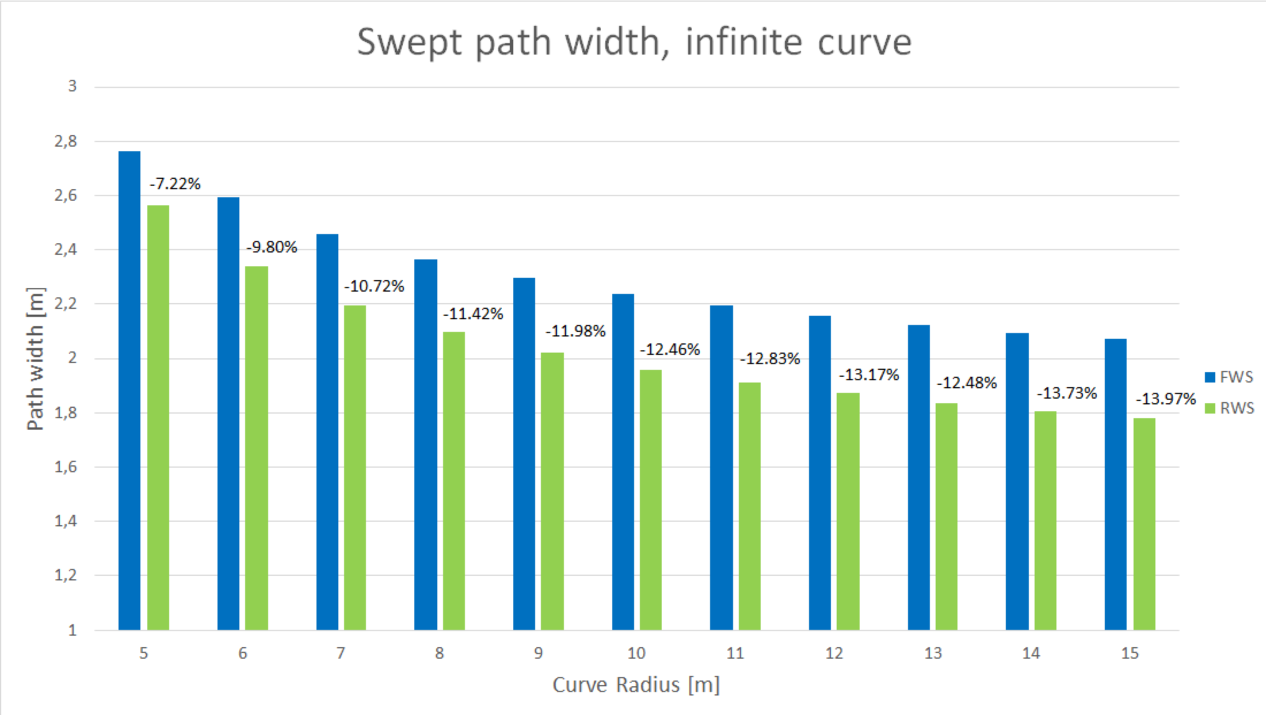

Figure 4.8: *Path width for different curve radii.*

The swept path width for different curve radii can be seen in figure 4.8. The vehicle with occupy the most space when following the smallest curve radius for both RWS and FWS. The reduction of swept path width is approximately 7.22% for RWS compared to FWS at 5m curve radius, and this reduction will increase as the curve radius increases. The change in percentage decrease over the spectrum of curve radii can be seen in figure 4.9 below.

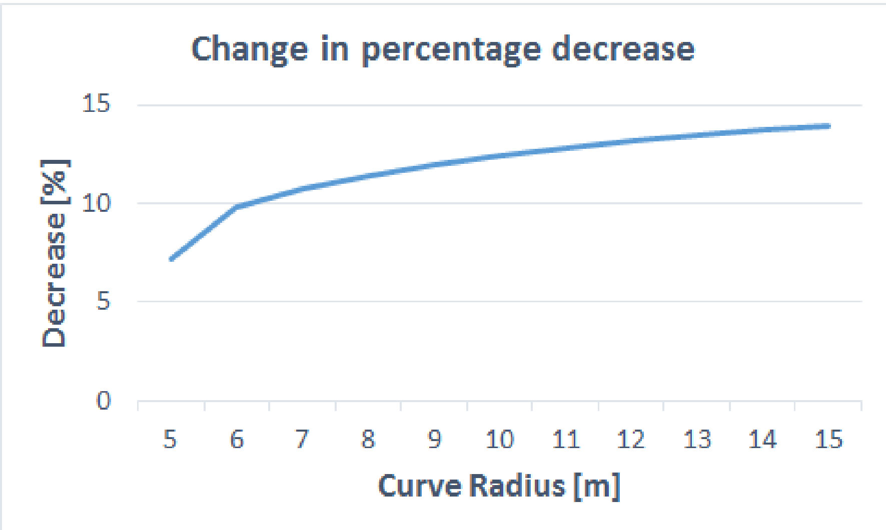

Figure 4.9: *Percentage decrease for increasing curve radii.*

The percentage decrease will have a declining increase as the curve radius grows larger.

The results from the driving scenarios can be seen below. Figure 4.10 shows the trajectory of the two most outer points on the vehicle driving through a T-crossing and the path that they trace out. As can be seen, the vehicle equipped with RWS (red line) has a narrower swept path width while turning and is intruding less in the opposite lane. The RWS vehicle will intrude 0.14m onto the opposite lane while the FWS vehicle will intrude 0.47m.

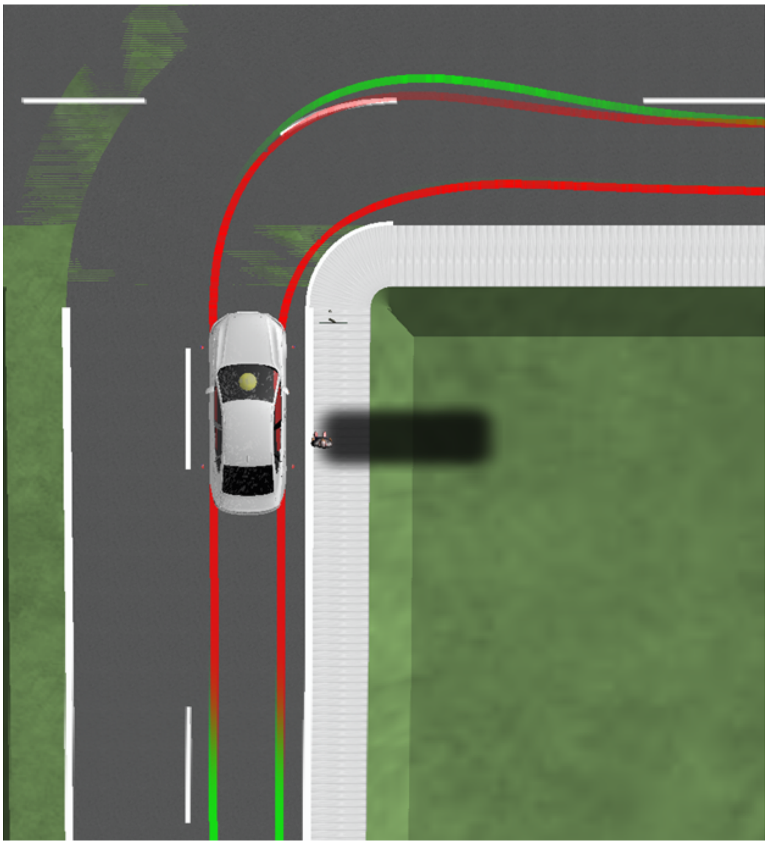

Figure 4.10: *Swept path for FWS (green) and RWS (red) driving through a T-crossing.*

Figure 4.11 shows the traced out path during a rear-end parking maneuver. The vehicle will initially turn to reach the right orientation, then stop, straighten the wheels out and reverse into the parking space. As can be seen in the figure, the vehicle equipped with RWS will take up less space than the vehicle with FWS only. The vehicle with RWS will manage the parking maneuver whereas the vehicle with FWS will not, and will intrude into the next parking space.

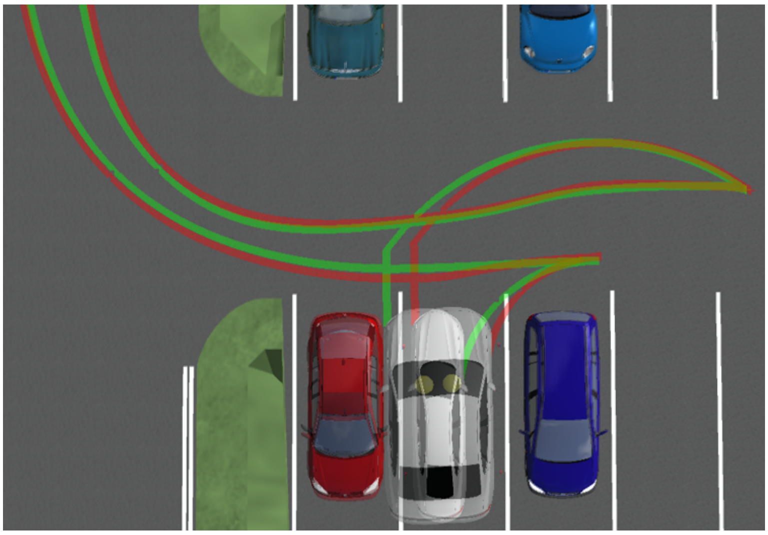

Figure 4.11: *Swept path for FWS (green) and RWS (red) for a parking maneuver.*

4.3 Highway lateral comfort

The results for highway lateral comfort during and overtaking and a sinus steer maneuver will be presented in this section. The results include yaw rate, lateral acceleration at CoG, body side slip angle and lateral acceleration at the passenger seat. A few tables are provided which reveal the weighed r.m.s. acceleration for comfort, the MSDV and the discomfort ratio between these values at CoG and at passenger and driver's seat respectively.

4.3.1 Frequency weighting

The frequency weighting for motion sickness in the lateral and vertical direction as well as for H&C in the horizontal plane can be seen in figure 4.12.

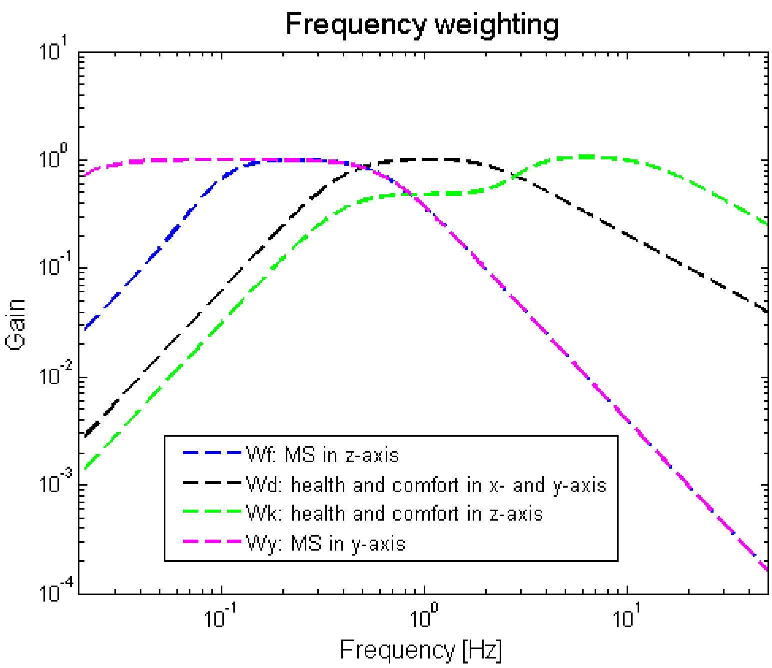

Figure 4.12: *Acceleration frequency weightings*

As can be seen in the figure, the weighting for motion sickness in the lateral direction is more sensitive in lower frequencies than the weighting in the vertical direction, as is supported by literature (Donohew and Griffin, 2004). The weighting for H&C in the horizontal direction is most sensitive around 1 Hz.

4.3.2 Overtaking

The yaw rate for both RWS controllers and FWS can be seen in figure 4.13 below. Comparing the RWS FB controller and FWS, one can see that there is not a large difference. The RWS FB controller has a slightly higher peak than FWS. The RWS FF controller has a slower response time and is lower, as was predicted by the step response.

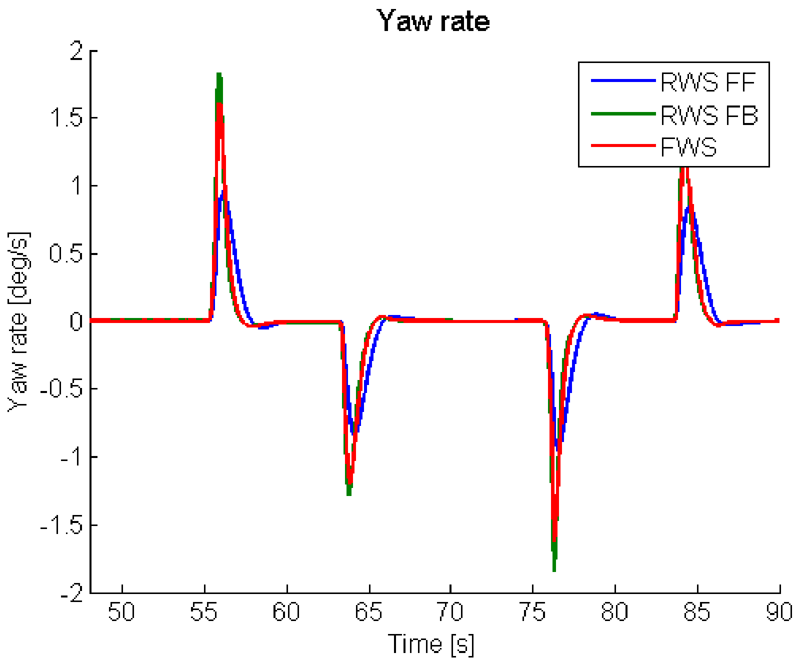

Figure 4.13: *Yaw rate for RWS FF (blue), RWS FB (green) and FWS (red) during an overtaking (90km/h).*

The lateral acceleration at CoG is approximately the same for RWS FB and FWS. The RWS FF controller produces and overall lower lateral acceleration.

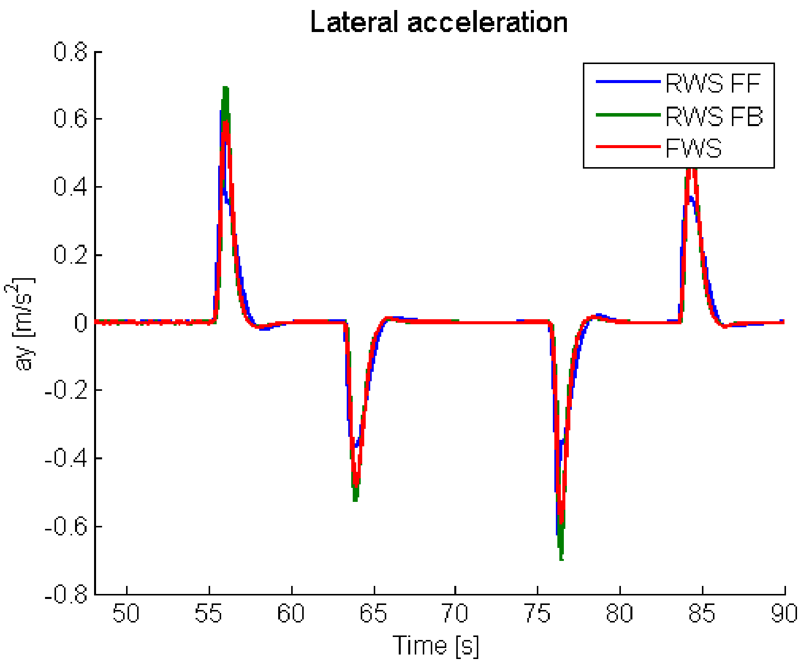

Figure 4.14: *Lateral acceleration at CoG for RWS FF (blue), RWS FB (green) and FWS (red) during an overtaking (90km/h).*

The body side slip angle is presented in figure 4.15. The side slip angle of the RWS FF controller is in the opposite direction from FWS and RWS FB controller. For a positive yaw rate there will be a positive body side slip angle for the RWS FF, and a negative angle for the other two configurations.

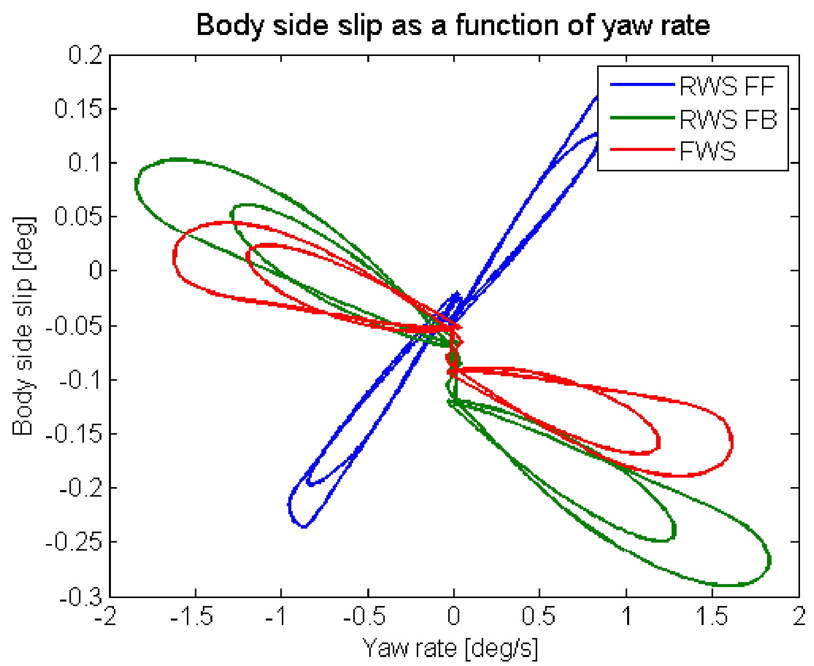

Figure 4.15: *Body side slip for RWS FF (blue), RWS FB (green) and FWS (red) during an overtaking (90km/h).*

The rear axle side slip can be seen in figure 4.16. The same pattern as for the yaw rate and lateral acceleration can be seen here. The RWS FB and FWS do not differ more than a small increase in RWS FB, and the RWS FF has the lowest rear side slip angle.

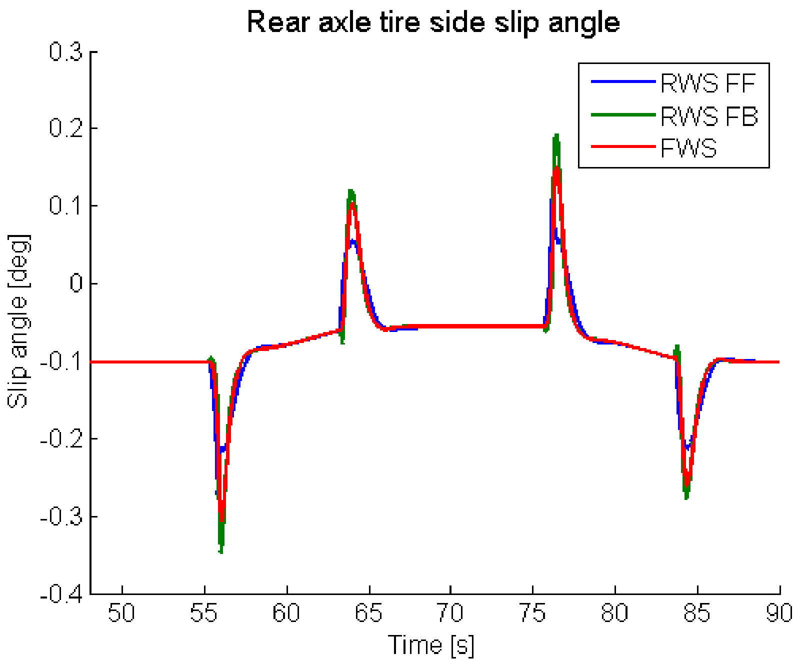

Figure 4.16: *Rear axle side slip for RWS FF (blue), RWS FB (green) and FWS (red) during an overtaking (90km/h).*

The steering wheel angle of the driver is presented in figure 4.17. As opposed to other measures, the RWS FF vehicle requires the greatest SWA during the maneuver. The RWS FB and FWS requires very similar SWA.

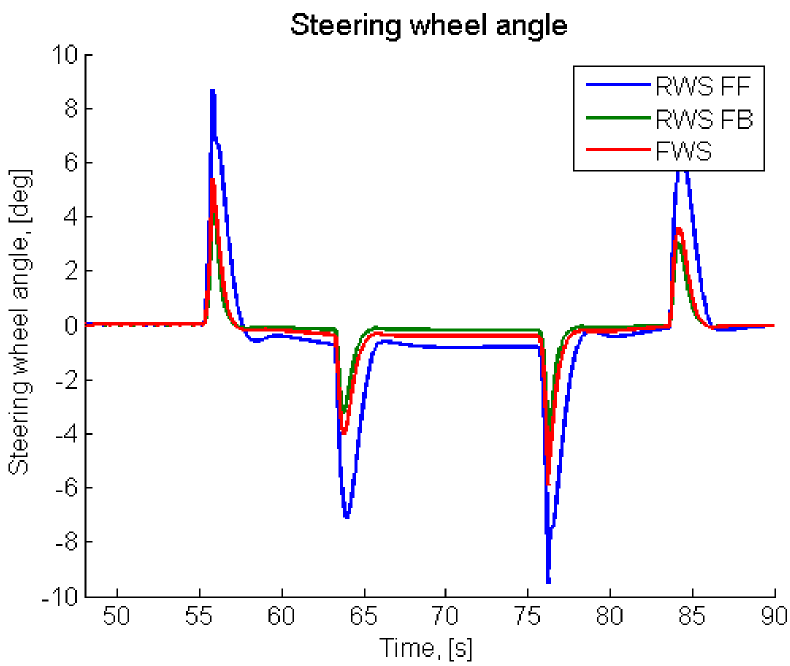

Figure 4.17: *Steering wheel angle for RWS FF (blue), RWS FB (green) and FWS (red) during an overtaking (90km/h).*

The lateral acceleration experienced by the occupants of a vehicle is presented in figure4.18. It is lower for RWS FF compared to the others. The configuration producing the highest occupant lateral acceleration is RWS FB. The acceleration experienced by the passenger is marginally greater than for the driver.

The jerk experienced by the occupants is seen in figure 4.19 below. The RWS FB produces the highest jerk

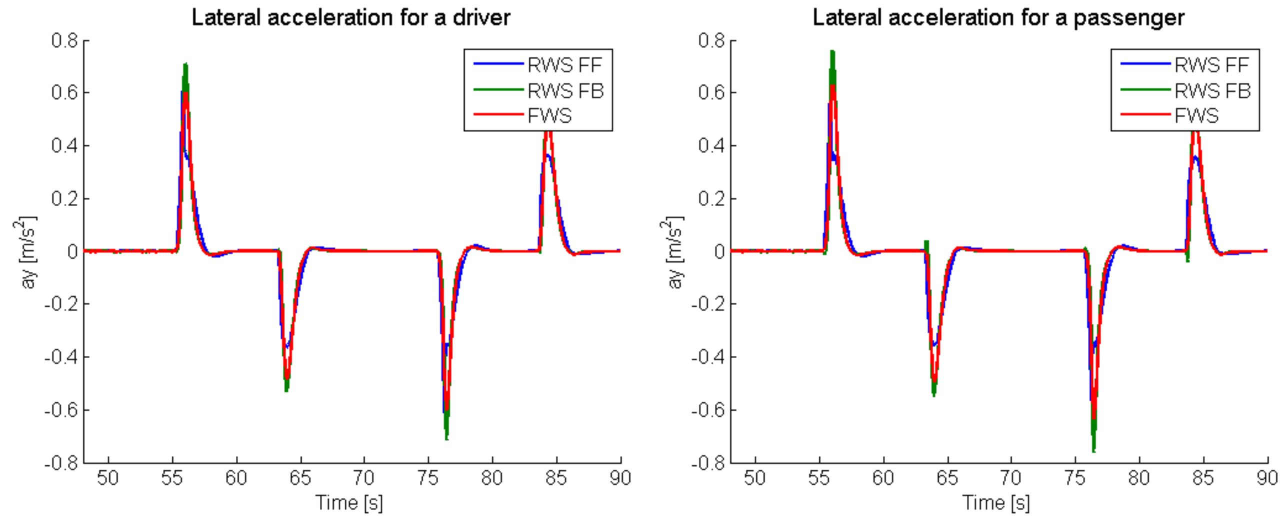

(a) *Driver.* (b) *Passenger.*

Figure 4.18: *Lateral acceleration experienced by occupants for RWS FF (blue), RWS FB (green) and FWS (red) during an overtaking (90km/h).*

values by far. The RWS FF has higher peaks than FWS but the duration is shorter. Here it is clear that the passenger experiences jerk of greater magnitude than the driver.

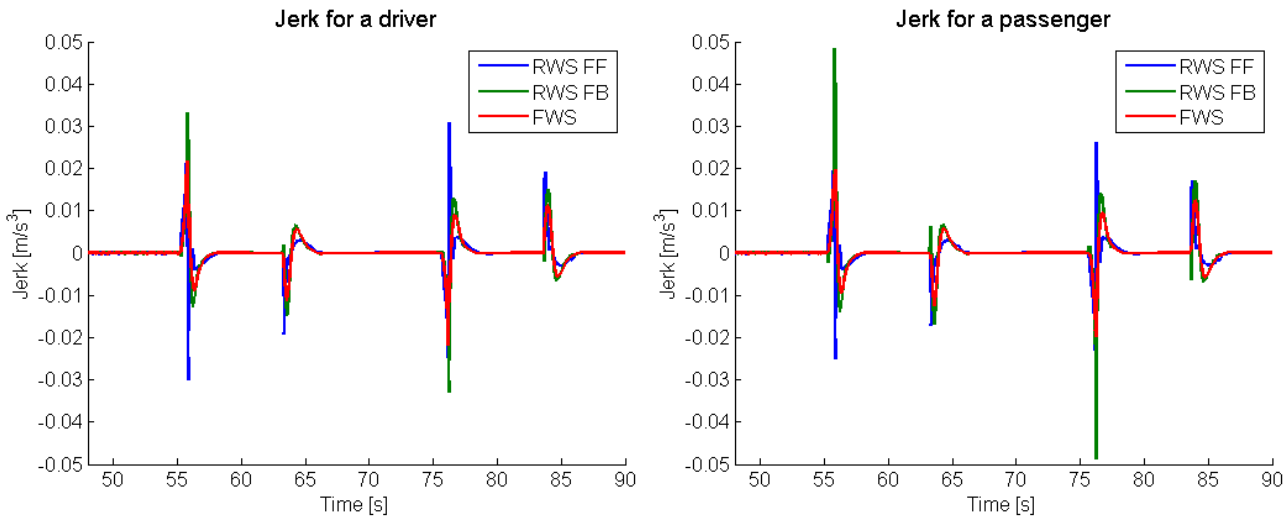

(a) *Driver.* (b) *Passenger.*

Figure 4.19: *Jerk experienced by occupants for RWS FF (blue), RWS FB (green) and FWS (blue) during an overtaking (90km/h).*

The discomfort ratios between driver/passenger and CoG for jerk r.m.s. and peak values are presented in figure 4.20 below.

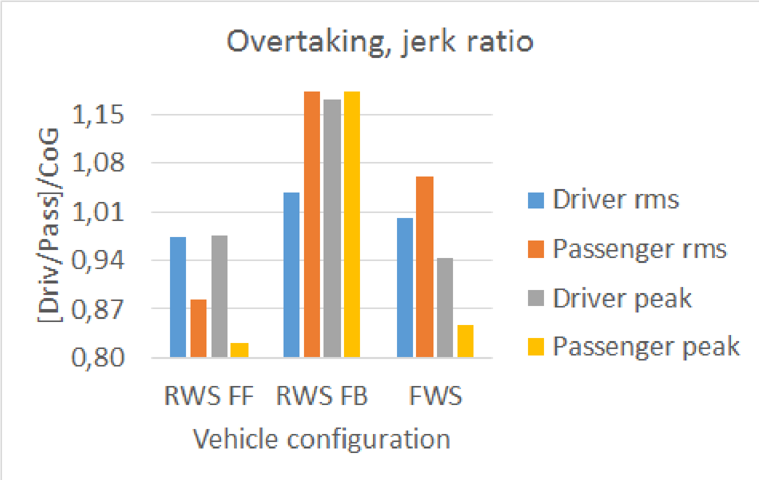

Figure 4.20: *Jerk ratio for overtaking.*

For the RWS FF controller, the peak jerk ratio is increased by 3.38% for the driver and decreased by 2.96% for the passenger compared to FWS. The r.m.s. jerk ratio is decreased by 2.76% for the driver and 16.68% for the passenger. For the RWS FB controller, the peak jerk ratio is increased by 24.01% for the driver and by 103.74% for the passenger compared to FWS. The r.m.s. jerk ratio is increased by 3.80% for the driver and 13.73% for the passenger.

The r.m.s. values for the W_d-weighted lateral accelerations can be seen in table 4.1. The values for RWS FF are lowest and the values for RWS FB are highest, in all positions. The change in driver and passenger seat compared to CoG is in the same direction depending on configuration. For RWS FF, both decrease compared to CoG, and for RWS FB and FWS they increase compared to CoG.

Table 4.1: Overtaking, a_y for comfort

	RWS FF	**RWS FB**	**FWS**
$a_{y_{CoG}}$	0.106	0.142	0.120
$a_{y_{driver}}$	0.102	0.146	0.122
$a_{y_{pass}}$	0.094	0.162	0.131

The values for MSDV can be seen in table 4.2. The RWS FF produces the lowest MSDV values and REW FB produces the highest. The change in driver's and passenger's seat compared to CoG is in this case also in the same direction; for RWS FF both decrease and for RWS FB and FWS they increase.

Table 4.2: Overtaking, MSDV

	RWS FF	**RWS FB**	**FWS**
$MSDV_{CoG}$	3.615	4.154	4.047
$MSDV_{driver}$	3.591	4.174	4.058
$MSDV_{pass}$	3.531	4.263	4.119

The discomfort and MSDV ratio can be seen in figure 4.21. As can be seen, the values for RWS FF are lower than 1 for both measures as opposed to RWS FB and FWS where the values are larger than 1. If the value is larger than 1 it implies that the acceleration at that point is larger than the acceleration at CoG, and if it is less than 1 it means that it is smaller than the value at CoG. Once more RWS FB produces the highest values.

For the RWS FF controller, the discomfort ratio is reduced by 4.19% for the driver and by 18.16% for the passenger, and the MSDV ratio is reduced by 0.94% for the driver and by 4.04% for the passenger compared to FWS. For the RWS FB controller, the discomfort ratio is increased by 1.89% for the driver and by 6.54% for the passenger, and the MSDV ratio is also increased by 0.35% and 1.47% for the driver and passenger

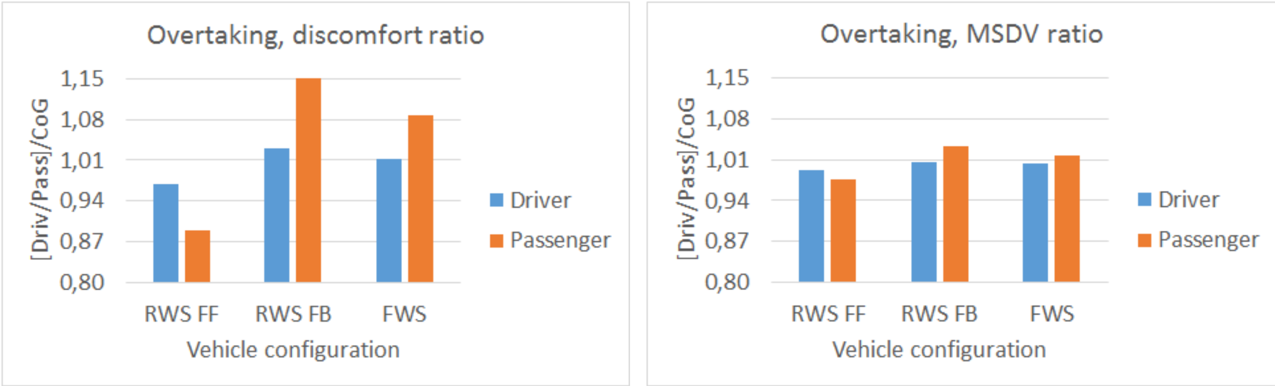

(a) *Comfort ratio.* (b) *MSDV ratio.*

Figure 4.21: *Discomfort and MSDV ratios for overtaking maneuver.*

respectively compared to FWS.

4.3.3 Sinus steer

The results from the sinus steer maneuver will be presented as r.m.s. values in bar charts rather than graphs as in the previous section. This is because the bar charts will present the results better in this case.

The yaw rate for the sinus steer maneuver can be seen in figure 4.22. As for the overtaking maneuver, the yaw rate for RWS FF is lower than for RWS FB and FWS. The difference between the two latter is smaller.

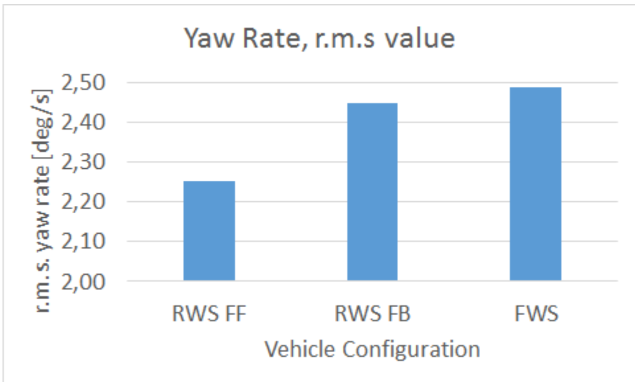

Figure 4.22: *Yaw rate for RWS FF, RWS FB and FWS during a sinus steer (0.2Hz, 90km/h).*

The lateral acceleration is approximately the same for all configurations as can be seen in figure 4.23.

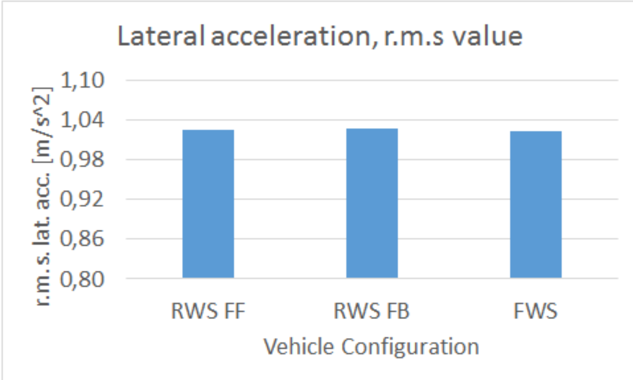

Figure 4.23: *Lateral acceleration at CoG for RWS FF, RWS FB and FWS during a sinus steer (0.2Hz, 90km/h).*

The body side slip angle as a function of yaw rate and in r.m.s. values can be seen in figure 4.24 below. The side slip produced with the RWS FF controller is in the opposite direction of the other two, as was the case for the overtaking maneuver as well. It is also about twice the magnitude. The side slip produced by the RWS FB controller follows the same direction as FWS but has a higher value.

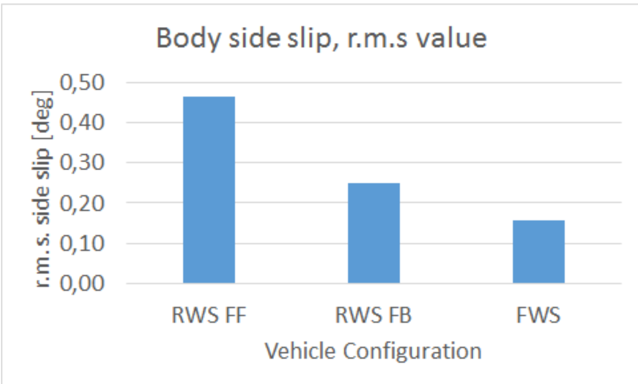

(a) *Body side slip r.m.s. values.*

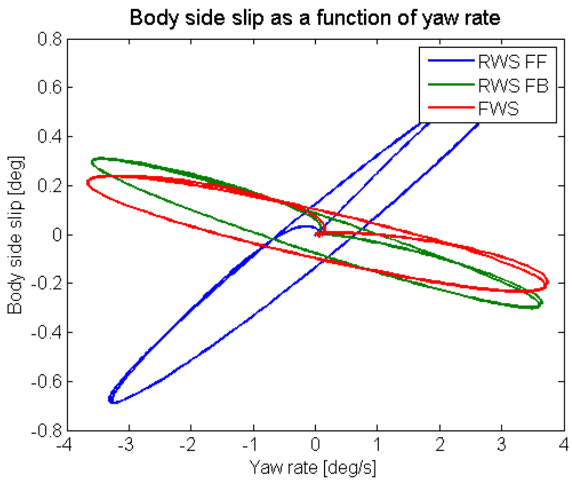

(b) *Body side slip as a function of yaw rate.*

Figure 4.24: *Body side slip during a sinus steer (0.2Hz, 90km/h).*

The rear axle side slip is presented in figure 4.25. Once more it is slightly lower for the RWS FF controller than for RWS FB and FWS, and the difference between the two latter is minor.

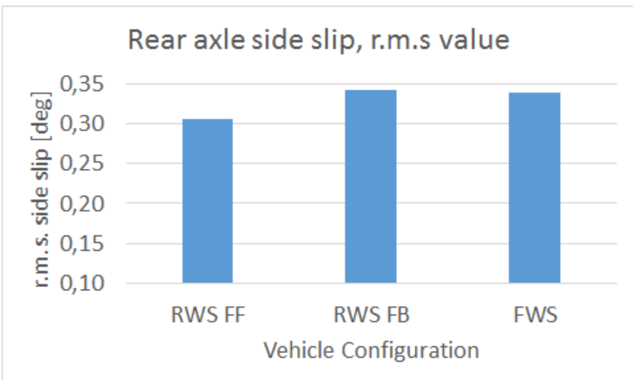

Figure 4.25: *Rear axle side slip for RWS FF, RWS FB and FWS during a sinus steer (0.2Hz, 90km/h).*

The steering wheel angle shows greater differences as can be seen in figure 4.26 below. The RWS FF requires the greatest SWA for the same maneuver and RWS FB requires a slightly lower SWA than FWS.

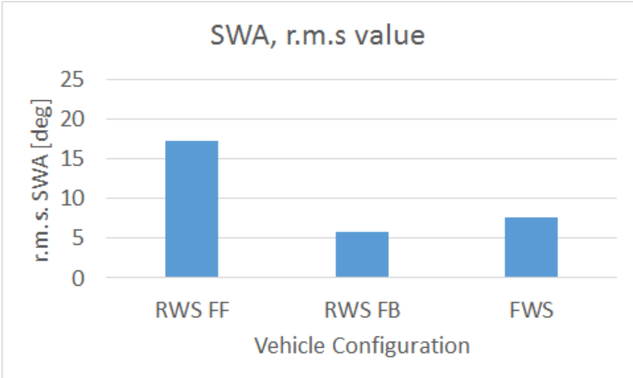

Figure 4.26: *Steering wheel angle for RWS FF, RWS FB and FWS during a sinus steer (0.2Hz, 90km/h).*

The lateral acceleration for the occupants, seen in figure 4.27, is lower for the RWS FF controller than for the other two. The RWS FB controller and FWS only have minor differences. It can also be seen that the driver experiences higher lateral acceleration than the passenger for all configurations, like in the overtaking maneuver.

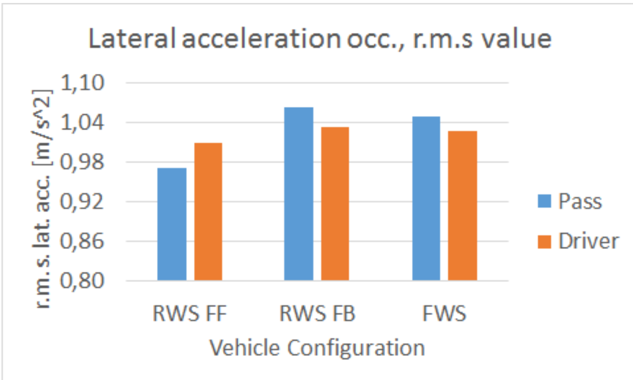

Figure 4.27: *Lateral acceleration for a passenger for RWS FF, RWS FB and FWS during a sinus steer (0.2Hz, 90km/h).*

The r.m.s. values for jerk can be seen in 4.28. The jerk for RWS FF is slightly lower and the jerk for RWS FB is slightly higher than for FWS, but the differences are small. It can be seen that the passenger experiences jerk of greater magnitude than the driver in all configurations but the RWS FF where the case is reversed.

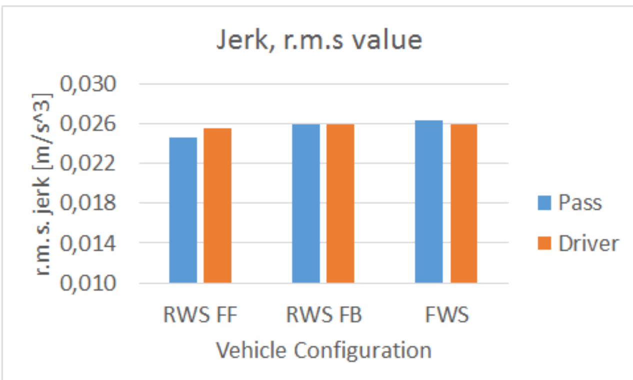

Figure 4.28: *Jerk experienced by the occupants for RWS FF, RWS FB and FWS during an overtaking (90km/h).*

In the following figures and tables, the results for the jerk, discomfort and MSDV ratio will be presented.

The discomfort ratio for jerk between driver/passenger and CoG can be seen in figure 4.29.

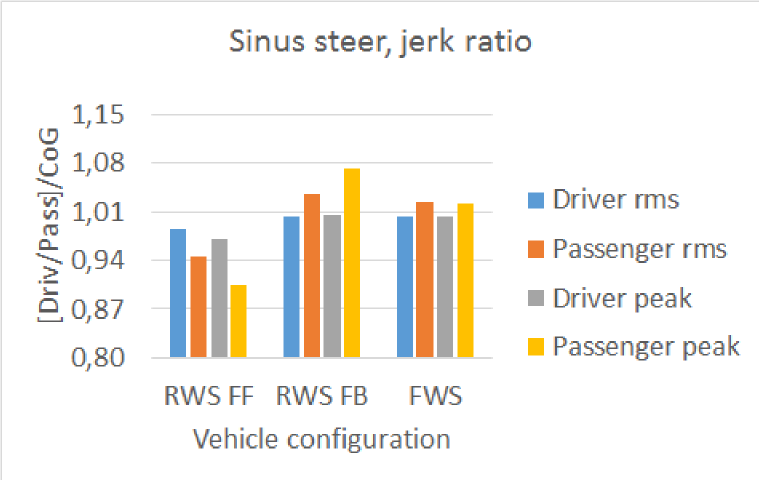

Figure 4.29: *Jerk ratio for a sinus steer maneuver.*

For the RWS FF controller, the peak jerk dicomfort ratio is reduced by 3.25% for the driver and 11.48% for the passenger compared to FWS. The r.m.s. jerk discomfort ratio is reduced by 1.92% for the driver and 7.54% for the passenger. For the RWS FB controller, the peak jerk discomfort ratio remains unchanged for the driver and is increased by 1.12% for the passenger compared to FWS. The r.m.s. jerk discomfort ratio is increased by 0.28% for the driver and by 5.03% for the passenger.

The r.m.s. value of the W_d-weighted lateral acceleration can be seen in table 4.3 below. The value highest at CoG is produced by RWS FF, but this configuration also produces the lowest value for the passenger. The valuees for the driver and passenger increase compared to CoG for RWS FB and FWS, and decrease for RWS FF.

Table 4.3: Sinus steer, a_y for comfort

	RWS FF	**RWS FB**	**FWS**
$a_{y_{CoG}}$	0.883	0.876	0.870
$a_{y_{driver}}$	0.868	0.881	0.874
$a_{y_{pass}}$	0.833	0.906	0.894

The MSDV follow the same pattern as the r.m.s. values above; there is a decrease in driver and passenger MSDV decrease for RWS FF compares to CoG, and increase for RWS FB and FWS. It is higher than for the overtaking maneuver as this maneuver is during a longer time period and is designed to trigger motion sickness.

Table 4.4: Sinus steer, MSDV

	RWS FF	**RWS FB**	**FWS**
$MSDV_{CoG}$	26.461	26.512	26.445
$MSDV_{driver}$	26.070	26.658	26.546
$MSDV_{pass}$	25.106	27.307	27.074

The discomfort ratio is presented in figure 4.30. Once more, the values produced by RWS FF is lower than 1 and the values produced by RWS FB and FWS are larger than one. The highest values belong to the RWS FB controller.

For the RWS FF controller, the discomfort ratio is reduced by 2.06% for the driver and by 8.17% for the

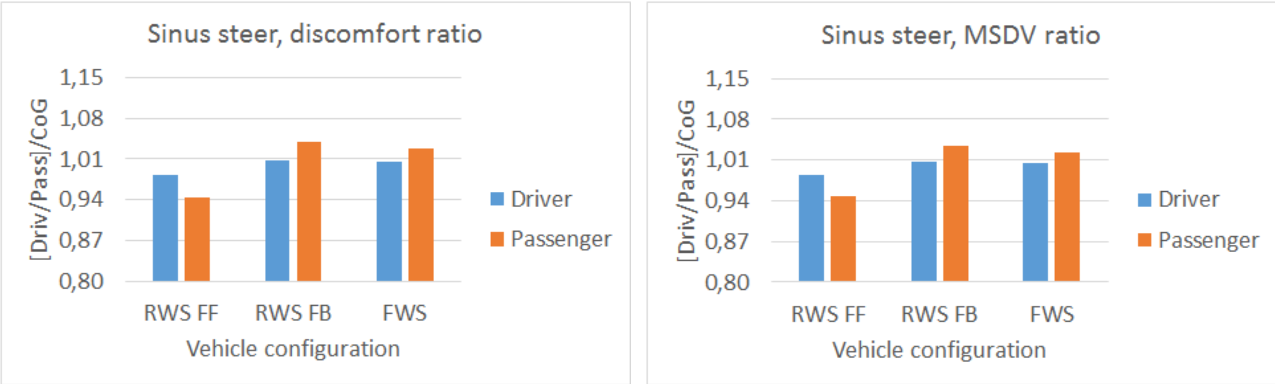

(a) *Comfort ratio.* (b) *MSDV ratio.*

Figure 4.30: *Disomfort and MSDV ratios for sinus steer maneuver.*

passenger, and the MSDV ratio is reduced by 1.85% for the driver and by 7.32% for the passenger compared to FWS. For the RWS FB controller, the discomfort ratio is increased by 0.36% for the driver and by 1.32% for the passenger, and the MSDV ratio is also increased by 0.31% and 1.12% for the driver and passenger respectively compared to FWS.

4.3.4 Yaw stability

The steering wheel angles producing 0.3g in 80km/h is presented in table 4.5 below. As can be seen the SWA is higher for the FF controller and lower for the FB controller compared to FWS.

Table 4.5: Steering wheel angles at 0.3g for 80km/h, SWD

	RWS FF	**RWS FB (10/25°/s)**	**RWS FB (40°/s)**	**FWS**
Clockwise	48.95°	21.78°	20.71°	25.40°
Counterclockwise	-49.16°	-21.23°	-20.76°	-25.50°

The FWS vehicle is able to handle the SWD maneuver in the clockwise and counterclockwise direction up to test 6, where is fails. Figure 4.31 shows the yaw rate for all different configurations during test 5 in the clockwise direction. As can be seen the yaw rate for the RWS FF controller has much greater phase lag than the others and doesn't reach as high peak. The RWS FB controller follows the yaw rate reference and returns to steady state faster than FWS.

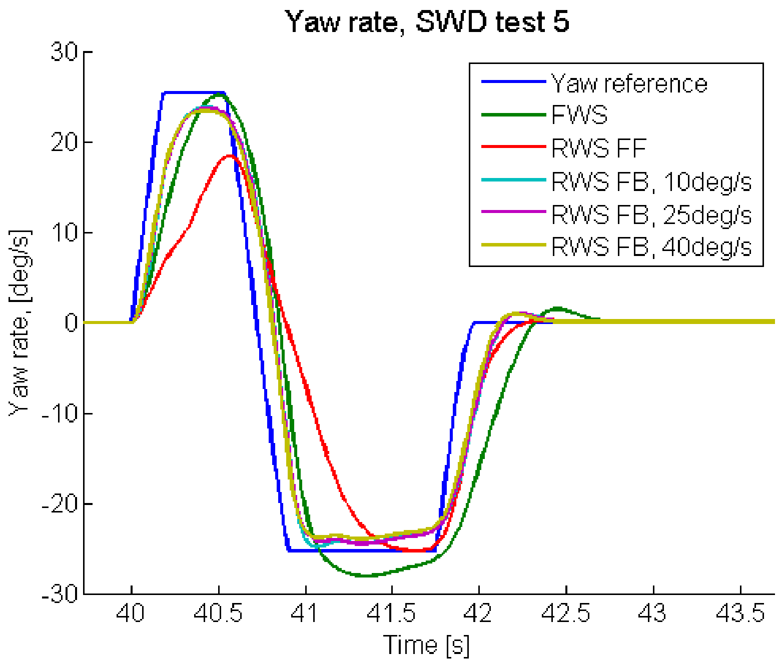

Figure 4.31: *SWD, test no 5.*

The RWS FF vehicle is able to handle the SWD maneuver up to test 11 in both clockwise and counterclockwise direction, where the maximum steering wheel angle of 300° is reached.

The RWS FB can reaches different tests depending on the rate of change of rear steer angle. If the angle rate on the rear wheels is limited to 10°/s, the vehicle can handle SWD up to test 6 in the clockwise direction and up to test 7 in the counterclockwise direction. If the rate is limited to 25°/s it reaches test 9 in both clockwise and counterclockwise direction, and if the rate is limited to 40°/s it reaches test 11 for both directions. If the rate of change on the rear wheel angle is unlimited, the vehicle will be able to perform all the tests in the series.

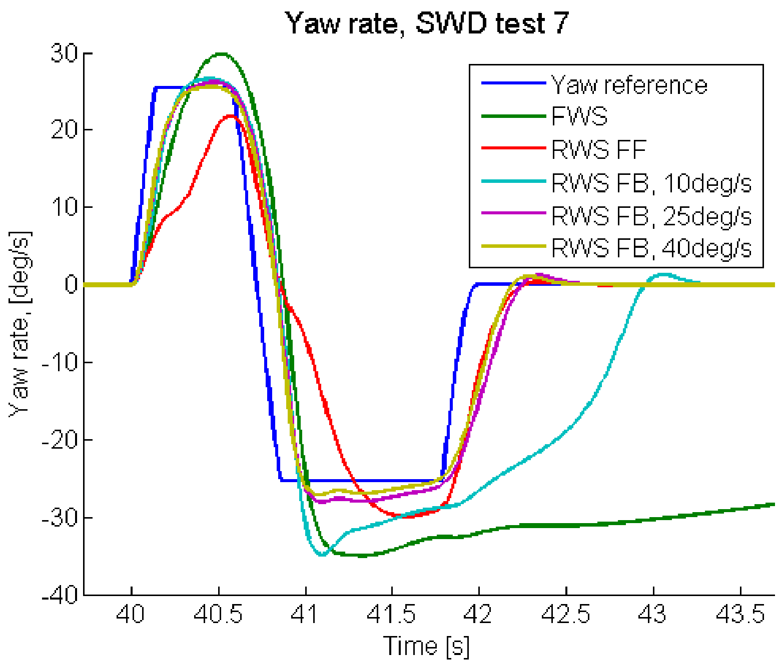

Figure 4.32: *SWD, test no 7.*

Figure 4.32 shows the yaw rate results for test 7 in the clockwise direction. The difference between the different rates of change is more prominent here. The controller with 10°/s rate of change is slower to respond to the second half of the period and reaches steady state later than the other two controllers with a rate of change of 25°/s and 40°/s. The difference between the two latter isn't as clear here but appears in following tests.

4.3.5 Driving simulator

The results collected from the motion platform are subjective only. Two professional test drivers as well as the author of this thesis drove the simulator at VCC equipped with the RWS FF controller. The vehicle has short roll transients in evasive maneuvers. The roll oscillations are dampened quite quickly and the vehicle reaches steady state. It is very unresponsive, there is a large phase lag present.

In slower maneuvers such as a lane change it was very smooth and the maneuver could hardly be felt. One could not tell that the vehicle was moving laterally apart from visual cues. The first steering input provided feedback and could be felt, but the second steering input as the vehicle straightens out in the next lane could not be felt as there is hardly any yaw. One test subject commented that it could imagine the vehicle being comfortable in lane changes as it doesn't have to take the eyes off the horizon.

The vehicle yaws a lot in low speed maneuvers, indicating high responsiveness.

5 Discussion

Simulation softwares such as CarMaker is highly useful in this kind of project. It is possible to recreate the exact same maneuver which is highly valuable for repeatability and quality of results. However, one should have in mind that some maneuvers possible to perform in the software is not possible in real life due to inconsistency in road conditions, wetness, wear etc. Some parameters such as road friction coefficient might have to be tuned in order to portray more realistic conditions and limit the performance of the virtual vehicle. This basic investigation has however shown the difference between using a vehicle with additional RWS and one with FWS only. Since no absolute values are required, only comparison, the software provides good results in this context.

As can be seen in figure 4.2, there seems to be a trade-off between yaw responsiveness and peak amplitude. The RWS FB controller produces a higher yaw rate as the reference yaw rate is less understeered than the modelled vehicle. According to the figure, the FB controller has a higher yaw acceleration as the yaw rate increases the fastest among the controllers, and thus the lateral acceleration outside the axis of rotation will be higher than for the other controllers. This is supported by the results for both comfort and MSDV as the FB controller produces the highest values. The characteristic response in lateral acceleration seen in figure 4.1 is due to the model and the fast increase in steering angle. The initial peak is a result of the wheels being turned instantly, and the slip develops after some time leading to a small decrease before the acceleration increases again. The RWS FB controller stands out among the two other configurations as it does not possess the same characteristic initial peak. The vehicle is initially understeered and as the controller is designed to follow a reference yaw rate, it will try to follow this rather than to build up lateral acceleration. Thus there seems to be a trade-off as the response in lateral acceleration is delayed with the gain of fast yaw rate response. One can clearly see the difference between the ideal and ISO step input. The ISO step input should be used as the ideal step input is only realizable in software, but not physically possible in reality.

The FF control law performs well both in lower speeds and in higher speeds. Figure 4.4 shows that the transition of wheel direction over the critical speed is smooth so that there will be no sudden changes that could ultimately lead to a dangerous situation. The effect of opposite steering directions is that the vehicle will act as a FWS vehicle with shorter wheelbase, making it able to follow tighter curves. The effect of the same steering direction is that the vehicle will act as a FWS vehicle with a longer wheelbase, making it more understeered and enabling smoother lateral movement. It does not have the same responsiveness for yaw rate as the FB controller as can be seen in both the step response (figure 4.2) and in the results for the two maneuvers. It does however dampen the peak amplitude which is good for comfort and motion sickness. However, it does not compensate for disturbances such as a side wind which the FB controller most likely will. The FB controller was tuned by trial and error in this thesis. Both the understeer and dampening coefficient, η and k_D, could be tuned by optimization for optimum performance. The FB controller could also be limited so that it is not active at all times but only in critical situations. There could for example be a yaw rate limit that would trigger the controller activation.

The rate limiters chosen were based on the findings of Håbring (Håbring, 2006). It can clearly be seen in figure 4.32 that there is a difference in controller performance when limiting the rate of change. This was also noted in how far the vehicle configurations got in the SWD testing sequence, where the controller with $40°/s$ performed the best. The actuator which used $10°/s$ did not improve the performance in the SWD test series, indicating that it is too slow to correct the yaw rate according to the reference. This result stresses the importance of quality of actuator responsible for turning the wheel. The choice of a slower actuator will affect the results considerably. The steering wheel angles were slightly different in the test series dependent on if it was steered clockwise or counterclockwise which is seen in table 4.5. Furthermore, some actuator and controller combinations performed better in one direction compared to the opposite direction (can be read in subsection 4.3.4). This could merely originate from asymmetry between the left and right side in suspension, steering, etc. The RWS FF controller is limited by the fact that the SWA is exceeding 300° which is a stopping limit for the SWD. This could be avoided by a changed steering ratio. By reducing the ratio, a smaller SWA would be needed for the same angle on the front wheels and thus the SWD could be further investigated for RWS FF. This is suggested for future work. An actuator with a rate of $25°/s$ was chosen for the comfort maneuvers and for the FF controller in both low- and high-speed maneuvers as this was recommended by Håbring (Håbring, 2006). In the future there could be a study in order to decide what the performance requirements of the system should be and decide upon an actuator accordingly.

One can clearly see where the angle of the rear wheels is saturated in figure 4.5. The difference in curvature between the four configurations stays approximately constant over the range of SWA. The results suggest that a vehicle equipped with RWS will be more maneuverable and responsive in low speeds as it can take tighter turns with a smaller SWA. The path width of the vehicle also supports this conclusion. The vehicle will take up less space when equipped with RWS and can thus enable better mobility in confined spaces. The difference in swept path width increases over the span of curve radii. The declination in the increase of percentage decrease suggests that there is a maximum decrease in swept path width at some point if the curve radius was to grow infinitely.

The T-crossing is a good example to asses how RWS could be used in more dynamic, low-speed maneuvers. It shows that a vehicle equipped with RWS will follow the corner better and not have as much overhang onto the opposite lane as a vehicle without, which reduces the risk for a collision with a vehicle coming from the opposite direction. As vehicles grow larger and there is more competition for space, it becomes more desirable for vehicles to take up less space which a vehicle equipped with RWS allows. However, one should have in mind if the angles on the rear wheels are too large, the rear of the vehicle could sweep out onto the opposing lane during the turn. The parking scenario is also a good example the practical use of RWS. Even though parking assistance systems are emerging, it is still useful for the driver to be able to park the vehicle in narrow spaces. Furthermore, the improved maneuverability of a RWS equipped vehicle is further supported by the fact that the entrance to the parking lot in the simulation had to be widened in order for the FWS vehicle to be able to enter.

Low speed maneuverability was assessed using the FF controller only. This is because the FB controller is not designed to improve low speed maneuverability, but to improve yaw stability. However, the choice of controller is less important in this aspect as the results suggest that RWS can improve maneuverability, which was the aim to begin with. In the future the controllers could be integrated to make it more universal.

The biggest challenge with evaluating comfort is that the vehicle is required to drive the exact same path at the exact same speed for the results to be directly comparable. Since this is very hard to achieve, even with a steering robot, the data for the passenger and driver is normalized using the data at CoG. Lateral acceleration at CoG is dependent on path and velocity according to

$$a_y = \frac{V^2}{R}$$

where V is the velocity and R is the curve radius. There is a difference in lateral acceleration at CoG which can be seen in 4.14. This suggests that the vehicles does not perform the same maneuver in the exact same way, calling for a need to normalize the data. the FF controller produces the lowest lateral acceleration for the driver and the passenger. It is lower for the two occupants than at CoG as opposed to the results for the FB controller and FWS where it is higher for the occupants than at CoG. The vehicle producing the highest values for lateral acceleration is the one equipped with the FB controller. This was mentioned earlier in the chapter and is a result of the increased responsiveness of the vehicle. One can see this in 4.19 where the jerk experienced by the passenger is displayed.

The results from the FF controller suggest that it is possible to improve comfort for a driver and a passenger by riding in a RWS equipped vehicle as the lateral acceleration that they are exposed to is lower in this vehicle configuration. The peak value of jerk are very low in magnitude, ranging from 0.02 to 0.05 m/s^3, thus being very far from the acceptable peak jerk value of 0.9m/s^3 (Eriksson and Svensson, 2015). The peak value for the driver is higher for the RWS FF controller than for FWS in the overtaking maneuver, which could be a result from the higher initial peak in lateral acceleration at the beginning of a steering input as could be seen in figure 4.1. However, the r.m.s. value of jerk is lower for the FF controller in both the sinus steer and overtaking maneuver. Thus future work calls for a developed method for evaluating the combined result of peak and r.m.s. jerk as it is complicated to asses the effect of them on comfort separately.

MSDV is also reduced for RWS FF compared to RWS FB and FWS. However, the evaluation of motion sickness is purely theoretical. The frequency weighting for lateral motion sickness has not yet been validated. However, since it builds upon the frequency weighting for motion sickness in the vertical direction, extending the sensitivity frequency range to include the lower frequencies where lateral motion causes motion sickness retains some of the validity. Furthermore, since jerk and lateral acceleration is reduced by the RWS FF controller, one could expect the relative motion between the eyes and a screen/paper/book to reduce as well which would reduce motion sickness according to Kato and Kitazaki (Kato and Kitazaki, 2006). To further evaluate if RWS can reduce motion sickness, an experiment needs to be performed in which a vehicle is driven the same path, in the same way, with and without RWS where the test subjects sit in the passenger seat and rate their experience. This could be done in a simulator or in reality. When performing these tests in the simulator however, one needs to eliminate the possibility of simulator sickness. This could be done by placing the subject in a confined space with no view of the road as this might trigger visually induced motion sickness.

The overtaking maneuver was chosen as this is a common maneuver performed on highways and was one were it was thought that RWS would improve the experience. The sinus steer was chosen as it is nauseating by personal experience and since literature uses lateral oscillation of varying frequency and magnitude. In the sinus maneuver, the r.m.s. values for comfort indicate that the ride was fairly uncomfortable to uncomfortable while the overtaking maneuver was classified as not uncomfortable according to ISO 2631 as can be read in section 2.1.2. Comfort and motion sickness should be further evaluated by driving for a longer period of time on a road that is specifically designed to be laterally uncomfortable. This road could be a digitalized model of a real road or a designed road with many different maneuvers.

The increase in steering wheel angle as could be seen in figures 4.17 and 4.26 in the results can become a problem for the driver as it has to steer more than it is used to, even more so at higher speeds. The difference in SWA in the overtaking maneuver results from that the road is not entirely straight, it is slightly curved. This challenge could be solved by using a feedback to the front wheels making them turn more without having to turn the steering wheel and without the additional front wheel steering from the feedback controller being fed back into the steering wheel. This would require steer by wire or any other technology which decouples wheel motion from steering wheel motion. However, if it was used in AD, it would be less of an issue as the driver is relieved to some extent of the steering responsibility. Steering corrections in AD tend to be quite fast even when driving on a straight. Thus it should be ensured that the RWS system can keep up with these fast corrections and not lag behind and lead to undesired behaviour. Furthermore, maneuvers at higher velocities are usually performed with smaller steering wheel angles and at a slower pace. One idea for future work could be to integrate rate of change of SWA in order for the system to understand when there is an evasive maneuver or not. For example, if the driver would turn the steering wheel fast, the system would be alerted of a possible dangerous situation and disconnect RWS. A RWS system that changes depending on situation could also be problematic as it would take longer for the driver to learn the behaviour of the vehicle.

The yaw rate is reduced for the FF controller because it does not fishtail as much as the FWS vehicle. This seems to be the main reason for the improvement of comfort as the vehicle does not rotate around its vertical axis as much with RWS, thus reducing lateral acceleration in positions outside of the axis of rotation.

Lateral acceleration at CoG is increasing slightly faster for the FF controlled vehicle compared to the other two as can be seen most clearly in figure 4.23. The reason for this could be that the vehicle does not have to turn its front, i.e. yaw, in order to move sideways since the wheels on both axles are turning at the same time. The rear end of the vehicle does not need to follow the front to the same extent as for FWS.

The side slip angle of the RWS FF equipped vehicle is much larger and in the opposite direction compared to FWS. As can be seen in figure 4.15 and 4.24, the RWS FF will produce a positive β for a positive yaw angle and the RWS FB and FWS will produce a positive β for a negative yaw rate. This means that the vehicle with RWS FF will understeer and the other two will oversteer. The RWS FB vehicle will ovesteer even more than the FWS vehicle. Understeering means that the side slip angle at the front axle will exceed that of the rear axle, and oversteering is vice versa. This can be seen in figures 4.16 and 4.25 where the rear side slip angle is less for RWS FF than for RWS FB and FWS. The cause could be that the rear wheels are not dragged along during RWS FF but actively turned. Understeering is generally desirable as it is deemed safer and more stable.

In this thesis, the two controllers were compared to an empty vehicle, i.e. a vehicle with no stability system. Both controllers outperformed the FWS vehicle in stability tests. However, since ESP is standard in all vehicle manufactured today it makes less sense to compare RWS to an empty vehicle only. Literature suggests both that ESP outperforms RWS on its own, and that stability can be further improved by using a combination of ESP and RWS. This should be further investigated in future work.

The simulator gave a good impression of how it feels to drive a vehicle with RWS. Something that has not been that investigated in this thesis is driver's comfort. This could be done in a simulator in the future.

6 Conclusion

Two control strategies were used, one feedforward control designed to keep the vehicle side slip angle zeroed at steady state cornering, and a feedback control take from literature designed to dampen yaw rate. The feedforward control's main usages were low speed maneuverability, highway lateral comfort and stability while the feedback control was designed mainly for stability.

The thesis was started with the aim to answer the following questions,

- How can highway lateral comfort be improved?
- How can low speed maneuverability be improved with RWS?
- What is the dynamic safety benefit with RWS?

A literature study was conducted in order to find measures of assessing vibration for comfort as well as motion sickness. Furthermore it was desired to find what motions causes motion sickness in vehicles. Comfort in its general term is usually associated with accelerations and jerks. Motion sickness is caused by low frequency oscillations increasing with increasing acceleration. The study resulted in a frequency weighting for comfort given by international standards, and a frequency weighting for motion sickness in the horizontal direction derived by Donohew and Griffin (Donohew and Griffin, 2000). It was also found that lateral motion is the primary cause of motion sickness in vehicles, namely lateral accelerations. The r.m.s. value of the weighed lateral acceleration was used as a measure of comfort and the MSDV was used as a measure of motion sickness. Thus the aim of the RWS control was to reduce lateral acceleration for passengers and drivers.

Two different scenarios were used for evaluating comfort; an overtaking maneuver and a sinus steer. The overtaking maneuver was used as it is a very common maneuver and the sinus steer was designed specifically to trigger motion sickness. The results suggest that the usage of RWS will decrease the discomfort ratio with 8.17% in the sinus steer maneuver and with 18.16% in the overtaking maneuver for a passenger in the rear seat as compared to a vehicle without RWS. The discomfort ratio will also decrease for the driver by 4.19% in the overtaking maneuver and by 1.85% in the sinus steer. Furthermore, both the peak and r.m.s. jerk discomfort ratios will decrease for a passenger in the rear seat by 2.96% and 16.66% respectively for the overtaking, and by 11.48% and 7.54% respectively for the sinus steer. The peak and r.m.s. jerk experienced by the driver will increase by 3.38% and decrease by 2.76% respectively for the overtaking maneuver, and decrease by 3.25% and 1.92% respectively for the sinus steer. A measure to combine the results peak and r.m.s. jerk should be searched for an used in future work. The results thus imply that the RWS equipped vehicle will be more comfortable to ride in as a passenger in the rear seat. The MSDV ratio is decreased by 7.32% in the sinus steer and by 4.04% in the overtaking maneuver for a passenger, and by 1.85% and 0.94% respectively for the driver, thus also indicating that motion sickness can be reduced with RWS. However, motion sickness also depends on view, personal experience and many other factors so the MSDV alone is not enough to assess motion sickness but it gives an idea about how the vehicle will affect motion sickness. Further studies need to be performed where test subjects are used to rate motion sickness and comfort in a vehicle with RWS and over a longer period of time. For example, a designed or existent road found to be laterally discomforting could be used. Furthermore, the results show that the comfort and MSDV improvements depend on where in the vehicle the occupant is seated and what maneuver is being driven.

Different measures of assessing low speed maneuverability was investigated; curb-to-curb, wall-to-wall and swept path width. The turning radius at CoG as well as swept path width was used as measures of maneuverability, as well as two driving maneuver to see how it can be used in practice. The results show that a vehicle equipped with RWS has a smaller swept path width, up to approximately 14% less in an infinite curve, indicating that it will occupy less space while being maneuvered compared to a vehicle with FWS only. Furthermore, the result show that the vehicle with RWS can perform more narrow turns for the same steering wheel angle compared to a FWS vehicle, also indicating improved low-speed maneuverability. The first driving maneuver involved a T-crossing where the vehicle stopped before performing the turn. The vehicle equipped with RWS was 0.14m into the opposite lane while the vehicle with FWS was 0.47m into the opposite lane. The second driving maneuver involved rear-end parking where it was shown that the vehicle with RWS could park without too much effort while the FWS vehicle parked onto the adjacent parking space.

The SWD maneuever was chosen to evaluate stability because it is designed to cause oversteering and is the maneuver which is used when assessing ESC systems. The results suggest that a vehicle equipped with RWS will improve stability as it can pass more tests in the SWD sequency than a FWS vehicle. It was also shown that the choice of actuator will affect the results considerably. There is a significant difference in performance when using the actuator with $10°/s$ and the one with $25°/s$. The difference is less between a $25°/s$ actuator and a $40°/s$, supporting the results of Håbring where it was concluded that an actuator of $25°/s$ would be sufficient for a RWS system. However, the FWS vehicle was not equipped with any stability system and thus a comparison to ESC could not be performed. For future work such a study should be conducted as an ESC system is standard by law in all new manufactured vehicles, and literature states both that ESC can be improved with RWS and that it cannot.

The thesis was started with the aim of investigating if RWS could improve low-speed maneuverability, highway lateral comfort and safety benefit in terms of stability. The results suggest that RWS is beneficial for all three aims. For the vehicle to be able to improve all three aims, the two controllers should be integrated. For low-speed maneuverability and highway lateral comfort, the FF controller is most appropriate. However, this thesis is merely a beginning of further studies in this field. There is more to explore and experience in this old, but new, technology which could lead to safer and more comfortable vehicles.

Bibliography

[1] Ackermann J, Sienel W, *Robust Yaw Damping of Cars with Front and Rear Wheel Steering*, IEEE Transactions on Control Systems Technology, Vol. 1, No. 1, 1993

[2] Besselink I, Veldhuizen T, Nijmeijer H, *Improving Yaw Dynamics by Feedforward Rear Wheel Steering*, Intelligent Vehicles Symposium, Eindhoven University of Technology, 2008.

[3] Bles W, Bos J E, de Graaf B, Groen E, Wertheim A H *Motion sickness: Only one provocative conflict?*, Brain Research Bulletin, Vol. 47, No. 5, pp.481-487, 1998.

[4] Bruzelius, F, *A theoretical justification of the sine with dwell manoeuvre*, Vehicle System Dynamics, 53:4, 493-505, 2015.

[5] Canale M, Fagiano L, *Comparing rear wheel steering and rear active differential approaches to vehicle yaw control*, Vehicle System Dynamics, 48:5, 529-526, 2009.

[6] Canale M, Fagiano L, *Stability control of 4WS vehicles using robust IMC techniques*, Vehicle System Dynamics, 46:11, 991-1011, 2008.

[7] Chatzikomis C I, Spentzas K N, *Comparison of a vehicle equipped with Electronic Stability Control (ESC) to a vehicle with Four Wheel Steering (4WS)*, Springer-Verlag Berlin Heidelberg, 2014.

[8] Da Silva M C G, *Measurements of comfort in vehicles*, Measurement Science and Technology, Vol. 13, No. 6, 2002.

[9] Diels C, Bos J E, *Self-driving carsickness*, Applied Ergonomics, 2015.

[10] Donohew B E, Griffin M J, *Motion Sickness: Effect of the Frequency of Lateral Oscillation* Aviation, Space and Environmental Medicine, Vol. 75, No. 8, 2004.

[11] Elbanhawi M, Simic M, Jazar R, *In the Passenger Seat: Investigating Ride Comfort Measures in Autonomous Cars*, IEE Intelligent Transportation Systems Magazine, 2015.

[12] Eriksson J, Svensson L, *Tunring for Ride Quality in Autonomous Vehicle: Application to Linear Quadratic Path Planning Algorithm* Examensarbete Uppsala Universitet, ISSN 1401-5757, 2015

[13] European Union, *Official Journal of the European Union*, L335, Vol. 58, 2015.

[14] Förstberg J, *Influence from horizontal and/or roll motion on nausea and motion sickness*, Swedish National Road and Transport Research Institute, VTI Rapport 450A, 2000

[15] Golding J F, *Motion sickness susceptibility*, Autonomic Neuroscience: Basic and Clinical 129 (2006) 67-76, Elsevier BV, 2006.

[16] Golding J F, Markey H M, Stott J R, *The effects of motion direction, body axis, and posture on motion sickness induced by low frequency linear oscillation*, Aviation, Space and Environmental Medicine, Vol. 66, No. 11, 1046-51 1995

[17] Håbring F, *Active Rear Wheel Steer Systems Analysis - An Actuator Requirements Approach*, Chalmers University of Technology, Master's Thesis 2006:30, 2006.

[18] Horiuchi S, *Evaluation of chassis control method through optimisation-based controllability region computation*, Vehicle System Dynamics, 50:sup1, 19-31, 2012.

[19] Huang Q, Wang H, *Fundamental Study of Jerk: Evaluation of Shift Quality and Ride Comfort* SAE International, ISSN 0148-7191, 2004

[20] IPG Automotive GmbH, *CarMaker, User's Guide*, 5.0.3, 2016.

[21] IPG Automotive GmbH *IPG Driver, User Manual*, 6.5, 2015.

[22] Swedish Standards Institute, *Vägfordon - Provningsmetoed vid lateral transientförhållande (undanmanöverprovning) - Open-loop.*, SS-ISO 7401:2011, IDT 2011

[23] International Organization for Standardization *Mechanical vibration and shock - Evaluation of human exposure to whole-body vibration.*, ISO 2631-1:1997(E), 1997

[24] Kato K, Kitazaki S, *A Study for Understanding Carsickness Based on the Sensory Conflict Theory*, SAE International, ISSN 0148-7191, 2006.

[25] Kreutz M, Horn M, Zehetner J, *Improving vehicle dynamics by active rear wheel steering*, Vehicle System Dynamics, 47:12, 1551-1564, 2009.

[26] Lennartson B, *Reglerteknikens grunder*, Studentlitteratur, 2002.

[27] Dobbs R, Smit S, Remes J, Manyika J, Roxburgh C, Restrepo A, *Urban world: Mapping the economic power of cities*, Report, McKinsey Global Institute, 2011

[28] SAE International *Taxonomy and Definitions for Terms Related to On-Road Motor Vehicle Automated Driving Systems*, SAE Information Report J3016, 2014

[29] Merriam Webster, *https://www.merriam-webster.com/dictionary/simulator*, accessed on 2017-01-15.

[30] Nagai M, Hirano Y, Yamanaka S, *Integrated Control of Active Rear Wheel Steering and Direct Yaw Moment Control*, Vehicle System Dynamics, 27:5-6, 357-370, 2007.

[31] Ogata K, *Modern Control Engineering*, Pearson Education Inc., 2010.

[32] Paillard A C, Quarck G, Paolino F, Denise P, Paolino M, Golding J F, Ghulyan-Bedikian V, *Motion sickness susceptibility in healthy subjects and vestibular patients: Effects of gender, age and trait-anxiety*, Journal of Vestibular Research Vol. 23, p.203-210, DOI 10.3233/VES-130501 2013

[33] Parsons K C, Whitham E M, Griffin M J, *Six Axis Vehicle Vibration and its Effects on Comfort*, Ergonomics, Vol. 22, No. 2, 211-225, 1979.

[34] Psychology dictionary, *http://psychologydictionary.org/gravireceptor-graviceptor/*, accessed on 2016-09-30.

[35] Sherman C R, *Motion Sickness: Review of Causes and Preventative Strategies*, J Travel Med, 9:251-256, 2002.

[36] Trafikverket, *Sektion tätort - gaturum.*, VV Publikation 2004:80, ISSN 1401-9612, 2004

[37] Trafikverket, *Vägutformning 94*, VV Publikation 2002:115, VU 94S-2, 2002.

[38] Turner M, Griffin M J, *Motion sickness in public transportation: the effect of driver, route and vehicle*, Ergonomics, Vol. 42, No.12, 1646-1664, 1999.

[39] United Nations, *World Urbanization Prospects: The 2014 Revision, Department of Economic and Social Affairs*, Population Division, 2015.

[40] Wembley Motors, *http://wembley-motors.com/eu-legislation-demands-esp-traction-control-systems-cars/*, accessed on 2016-12-15.

[41] Wikiwand, `http://www.wikiwand.com/de/Wendekreis_(Fahrzeug)`, accessed on 2016-10-14.

[42] Yim S, *Coordinated control with electronic stability control and active steering devices*, Journal of Mechanical Science and Technology 29 (12), 5409-5416, 2015.

[43] Zhang L-L, Wang J-Q, Qi R-R, Pan L-L, Li M, Cai Y-L, *Motion Sickness: Current Knowledge and Recent Advance*, CNS Neuroscience & Therapeutics 22 (2016), 15-24, 2015.

A Simulink: Feedforward model

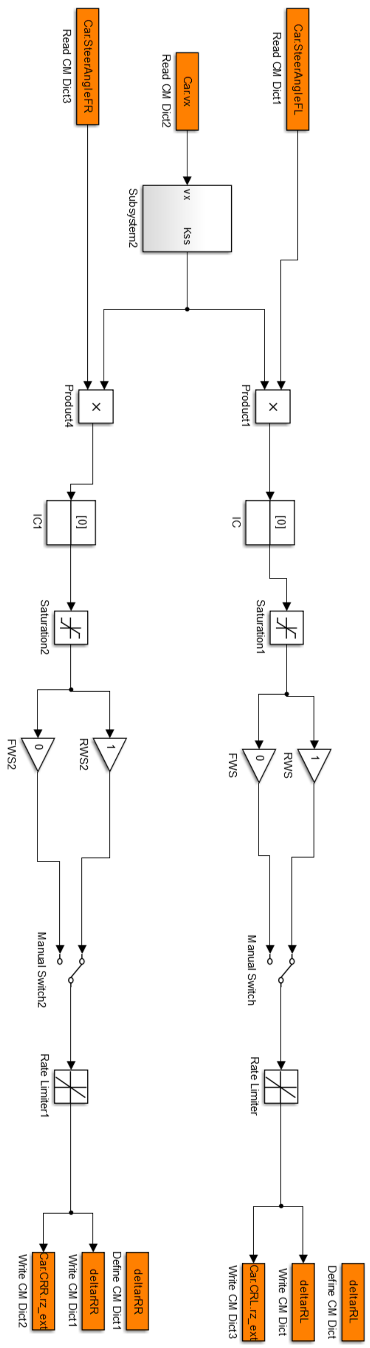

B Simulink: Feedback model

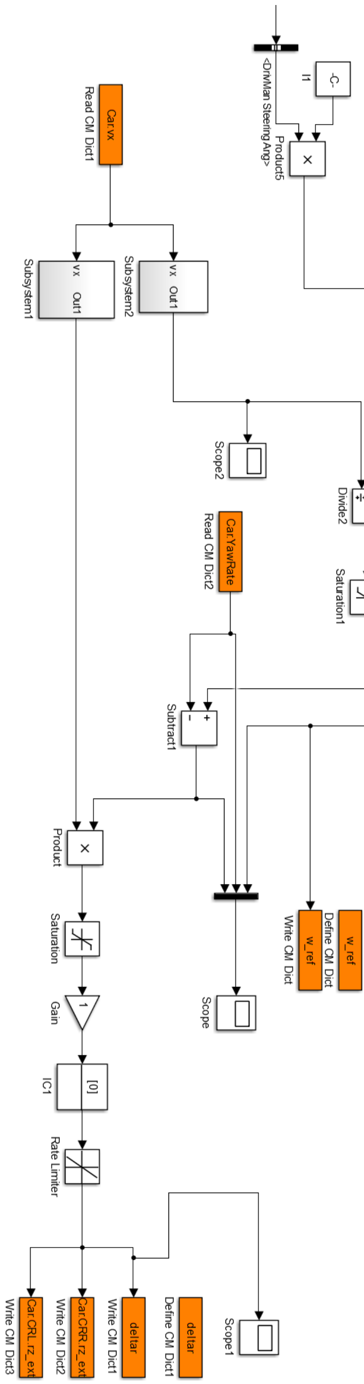

C ISO-standard frequency weighting W_d

Table C.1: Parameters for W_d

Band-limiting			a-v transition			Upward step				
f1	Q1	f2	Q2	f3	f4	Q4	f5	Q5	f6	Q6
0.4	$1/\sqrt{2}$	100	$1/\sqrt{2}$	2.0	2.0	0.63	∞	-	∞	-